university of groningen

faculty of science and engineering

Observation of Double Electron Capture by Sn Ions from H_2 Using Reaction Microscopy

Symen Schilstra

university of groningen / faculty of science and engineering

University of Groningen

Credit Assignment for Surrogate Gradient Learning Rules in Spiking Neural Networks

Master's Thesis

To fulfill the requirements for the degree of
Master of Science in Applied Physics
at University of Groningen under the supervision of
Prof. dr. ir. R. Hoekstra (Quantum Interactions and Structural Dynamics, University of Groningen)
and
E. de Wit (Quantum Interactions and Structural Dynamics, University of Groningen)
Second examination preformed by
Dr. T.A. Schlathölter (Quantum Interactions and Structural Dynamics, University of Groningen)

Symen Schilstra (s3789462)

April 19, 2024

Contents

Acknowledgments

I would like to thank the entire QISD group. I have had a great time in the group discussing physics and overcoming technical challenges during the project. It was a great experience where I learned a lot about different kinds of lab work. I was not used to actually installing and discovering how to use new lab equipment like done in this project. All I had done before was simply using the equipment that had already been used in research for considerable amount of time. This lab gave me much more inside about what actually goes into conducting scientific research. The most interesting part of the project was actually getting to the first data and coming up with explanations for the observed phenomena followed by thinking of ways to extract information out of them. I would like to offer special thanks to Emiel de Wit for assisting me for the entirety of the project, Mart Salverda for all the technical help and explanations, Ronnie Hoekstra for the discussions about the project and for allowing me to do my master thesis in his research group and Thomas Schlathölter for being my second examiner. I would also like to thank the other master students in particular Lennart Tinga and Thomas Nieboer for the discussions and assistance during many parts of the research.

Abstract

Ion interactions are an interesting subject to study due to their relevance in state of the art EUV lithography machines. ASML is a major player in the semiconductor industry because they are able to produce machines that produce the smallest features on wavers. ASML is always trying to further optimise and comprehend the processes taking part in their machines. This paper looks into the effect of hydrogen on moving tin ions. This is relevant because ASML has a tin plasma in their most recent machines that produces the extreme ultra violet light used for the lithography. This tin plasma also produces tin ion projectiles that should not interfere with the rest of the machine. Hydrogen is used to protect the machine and transport the tin away. This paper looks into a measurement apparatus that will be able to determine the energy release as a consequence of double capture charge transfer of tin ions from molecular hydrogen. Previous work has been done on the subject which revealed inconsistencies in the results for Sn^{3+}. This setup will be able to give more insight in these processes. The device is a reaction microscope which allows us to take Time of Flight(ToF) and position data at the same time. The aim of this project is to establish a basic functioning of the device and to acquire and analyse first data. The focus in this thesis will lay on the analysis and will be concluded with recommendations and outlook for the project. We can conclude that the reaction microscope is operational and has provided valuable data. The double capture observed shows 9.7 eV hydrogen fragments as theory suggests. The reaction microscope will have to be improved further but shows great promise.

1 Introduction

With the growing demand of computing power globally more and better computer chips are needed. ASML is a mayor factor in the microchip industry. ASML produces machines that make computer chips. They are the leader in the their field allowing production of the smallest features ever. Their most recent Extreme Ultra Violet high NA machine allows for a Critical dimension of 8 nm, an incredible feat. ASML is always looking to increase their machines performance and efficiency which is the reason this research is conducted.

The EUV machines of ASML use tin to create EUV light. They hit tin droplets with a high power laser which causes the tin to become a plasma. Electron transitions in the plasma create the EUV light. The plasma disperses around the vacuum chamber when hit by the laser in the form of ions. To protect the machine and its delicate equipment a hydrogen gas is introduced to protect the inside of the machine, like mirrors. The downside of using this hydrogen gas is that the gas will absorb part of the EUV light. It is thus important to determine how much hydrogen would be needed to protect the machine. To determine this the Sn ion H_2 gas interactions will have to be understood. Previous work by S.Rai[1] has already shown that for a particular charge exchange interaction, double capture, Hydrogen fragments generally receive 9.7 eV kinetic energy. However an inconsistency was found when using Sn^{3+} 48 keV as a projectile ion. The energy was now lower. To look further into this phenomena we constructed a reaction microscope. Preliminary work in the form of simulations of the system and establishing equations have been done by R. Julius[2].

This thesis will focus on the installation and first data of a reaction microscope which will be used to determine an energy profile of double electron capture of two electrons of hydrogen gas by Sn^{6+} and He^{2+} ions. A reaction microscope is a device that utilises electric fields to accelerate charged particles to a detector. The detector will record both the time of flight and position data of incoming particles which can later be used to determine various properties of a sample. This thesis contains a short introductory theory section with the main focus being the trajectories of ions. An experimental setup section where the setups and the detector are discussed. First data with the reaction microscope is acquired and discussed in the results section. The conclusion section highlights the main findings, recommendations and options for further research.

2 Theory

We want to facilitate the stopping of Sn highly charged ions. To accommodate this hydrogen is used. The interactions between hydrogen and tin ions are therefore highly interesting.

2.1 Electron capture/Charge exchange

When a positive ion is in a suitable range to a hydrogen atom an exchange interaction can occur. There are many possible types of these interactions but the most important part of these reactions is that H^+ with 9.7 eV kinetic energy can be formed. The other possible hydrogen products are H_2^+ with 0 eV kinetic energy and H^+ with 0 eV kinetic energy. The most notable reactions in the case of Sn ions are depicted below.

one electron capture

$$Sn^{q+} + H_2 \rightarrow Sn^{(q-1)+} + H_2^+ \tag{1}$$
$$Sn^{q+} + H_2 \rightarrow Sn^{(q-1)+} + H^+ + H \tag{2}$$

autoionizing double capture

$$Sn^{q+} + H_2 \rightarrow Sn^{(q-1)+} + 2H^+ + e \tag{3}$$

bound double capture

$$Sn^{q+} + H_2 \rightarrow Sn^{(q-2)+} + 2H^+ \tag{4}$$

Both the double capture reactions lead to two H^+ particles which will mean repulsion of these two positive particles, also called a coulomb explosion. In figure 1 we see how this process works.

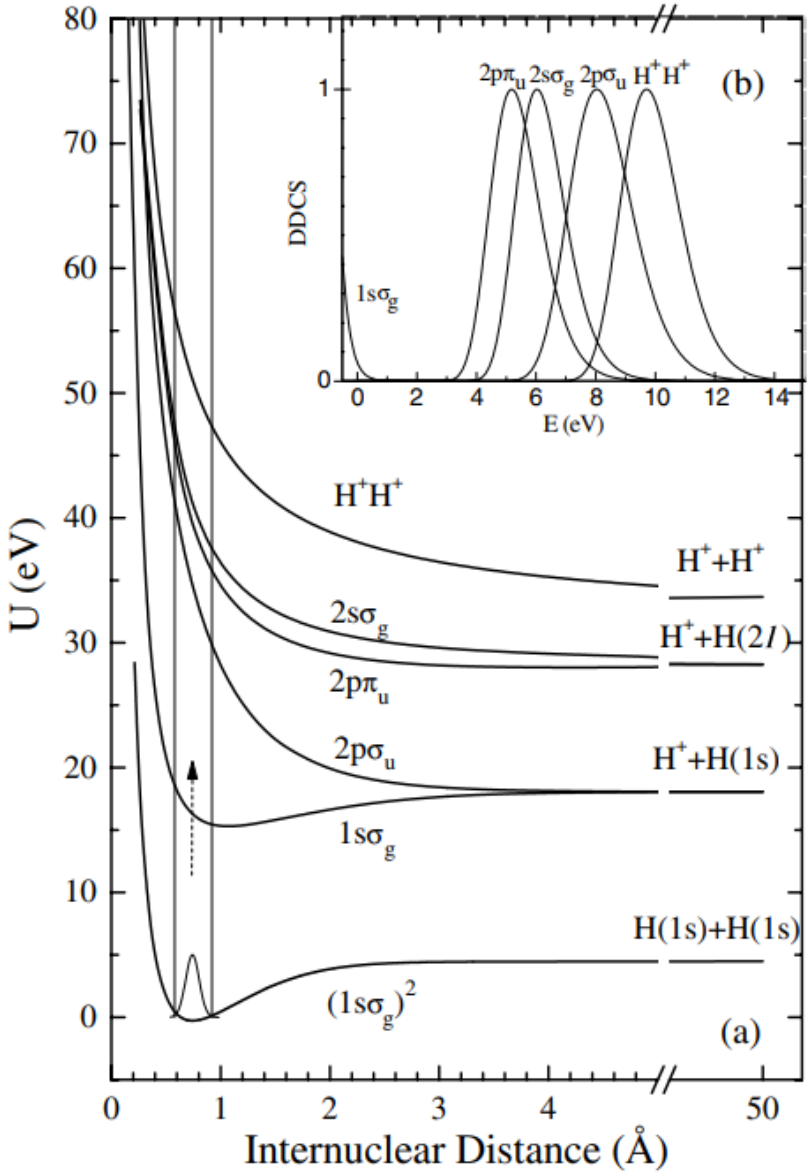

Figure 1: (a) Potential energy curves for selected states of H_2, H_2^+ and H_2^{2+}[3].
(b)Predicted fragment energy distributions based on the Franck–Condon model and corresponding to the states in (b). Image taken from [4]

The transition probability of H_2 transitioning to $2H^+$ is determined by the overlap between the bound vibrational state of the nuclei and the wavefunction in the continuum as the Franck-Condon principle entails[4]. The bottom state shows the potential well that corresponds to H_2. If the hydrogen loses both electrons it will move up to the potential denoted as H^+H^+. This potential will make the two particles separate by a coulomb explosion. The difference between the potential at infinity and the value attained during the transition to the potential will be half of the kinetic energy both the hydrogen atoms attain. The inset (b) shows that the most probable energy of H^+H^+ is 9.7 eV and that the distribution of possible energies is fairly wide, extending over 20% of the most probable value. For further information about these process and assumptions see[3][4].
The one electron capture reaction can produce H_2^+ This will have close to 0 eV kinetic energy.
$H^+ +$ H Could have multiple different energies as can be seen in figure1. These are not very prevalent

interaction pathways we assume. We do however know that 0 eV H^+ is also a possible result but the exact origin of these is unknown[1]
most important part of this section is to distinguishing that H^{2+} fragments have low energy around 0 Ev and that H^+ fragments can have relatively high energy around 9.7 eV and also 0 eV.

2.2 Trajectories

The trajectories and the expressions that govern them are of vital importance for interpreting data and thus should be discussed.

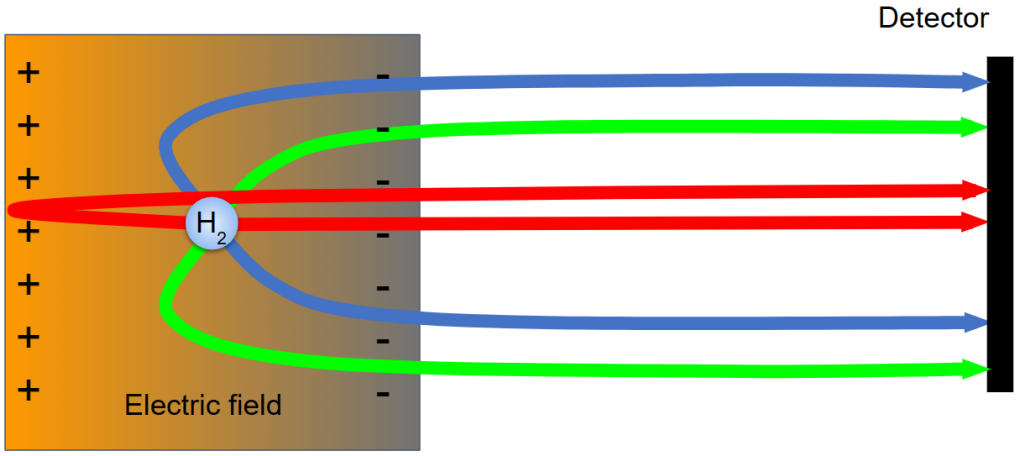

Figure 2: Schematic representation of trajectories of H^+ following a coulomb explosion. The ions are accelerated by an electric field followed by a flight tube and lastly collected on a detector. Every color corresponds to the trajectories of a single pair of hydrogen atoms that repulse each other

Most of the equations that are useful for this research are about the trajectories due to an electric field we apply. The hydrogen fragments are produced by an ion bunch interacting with molecular hydrogen gas. The region where this interaction occurs is called the interaction region and is depicted in figure 2 as a H_2 circle. If single electron capture occurs no energetic fragments are produced. These fragments will simple be accelerated by the field straight towards the detector. If double electron capture occurs the fragments receive the 9.7 eV kinetic energy as discussed before. These particles will therefore show trajectories that allow them to appear on different locations on the detector. Figure 2 shows some possible trajectories of these ions. The red color depicts the trajectory of a particle pair with momentum parallel to the normal of the detector. The other colors represent particle pairs with momentum both parallel and perpendicular to the normal of the detector. The equations that are used in data analysis are shown below
The force, F_a on a recoil ion can be calculated with

$$F_a = q_r E_a \tag{5}$$

where q_r is the charge of the recoil ion and E_a is the strength of the electric field
Newton's second law of motion states

$$F_a = m_r a_a \tag{6}$$

Where m_r is the mass of the recoil ion and a_a the acceleration of this ion due to the electric field.
Combining equations 5 and 6 we obtain

$$a_a = \frac{q_r E_a}{m_r} \tag{7}$$

The kinetic energy of a particle is

$$E = \frac{1}{2}mv^2 \tag{8}$$

The distance travelled away from the interaction region in the direction of the detector normal is given by

$$D = vt - \frac{1}{2}a_a t^2 \tag{9}$$

The energy of the hydrogen particles can be broken down into two parts, $E_{\parallel}$ and $E_{\perp}$

$$E_{total} = E_{\parallel} + E_{\perp} \tag{10}$$

$$E_{\perp} = E_{total} - E_{\parallel} \tag{11}$$

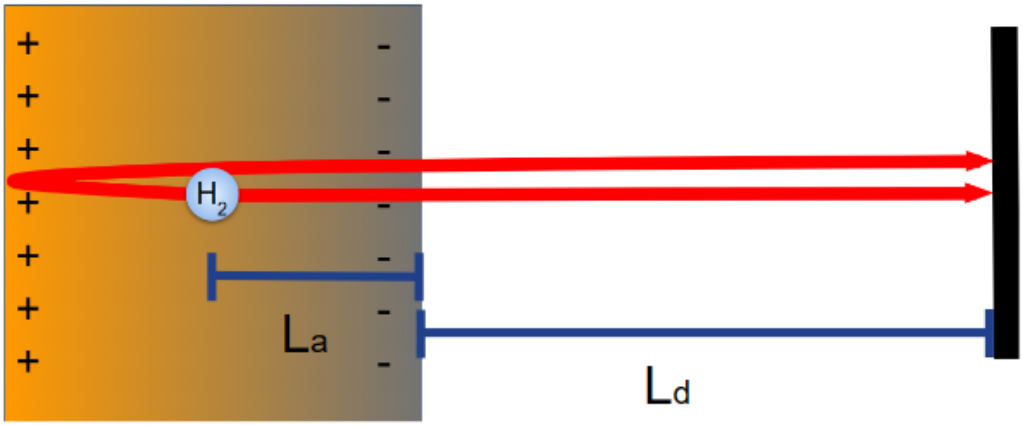

Figure 3: Schematic representation of trajectories of H^+ following a coulomb explosion. The parameters L_a and L_d are shown

If we would like to know the position of where the fragments will intersect the detector we can utilise the equation below

$$R\pm = \sqrt{E_{\perp}}\left(\frac{2L_a}{\sqrt{E_{\parallel} + q_r E_a L_a} \pm \sqrt{E_{\parallel}}} + \frac{L_d}{\sqrt{E_{\parallel} + q_r E_a L_a}}\right) \tag{12}$$

where $R\pm$ are the two fragment positions on the detector taking the origin of the fragments as 0. L_a is the distance from the origin of the particles to the edge of the acceleration region and L_d is the length of the flight tube as can also be seen in figure 3. If we add both of the solutions together and use equation 11 we can construct an equation that gives the distance between the two particles, Δr

$$\Delta r = \sqrt{E_{total} - E_{\parallel}}\left(\frac{4L_a\sqrt{E_{\parallel} + q_r E_a L_a}}{q_r E_a L_a} + \frac{2L_d}{\sqrt{E_{\parallel} + q_r E_a L_a}}\right) \tag{13}$$

The time between when the first and the second particle hit is given by Δt

$$\Delta t = \frac{\sqrt{8m_r E_{\parallel}}}{q_r E_a} \tag{14}$$

The total time of flight for both of the particles will be given by

$$t_{ToF}\pm = \sqrt{\frac{m_r}{2}}\left(\frac{2L_a}{\sqrt{E_\parallel + q_r E_a L_a} \pm \sqrt{E_\parallel}} + \frac{L_d}{\sqrt{E_\parallel + q_r E_a L_a}}\right) \tag{15}$$

For the derivation of equations 12, 14 and 15 see the master thesis of Robbert Julius [2]

Robbert Julius has simulated many possible configuration and spectra in his thesis[2]. It shows that if the interaction region is assumed to be small and the field is homogeneous the position spectra will look like figure 4. The red color indicates the position the ions will hit on the detector for that specific ToF window. We can see that the low ToF starts of as a dot. This is the case because these are H^+ emitted straight towards the detector. Particles with more sideways momentum will reach the detector a bit slower increasing the ToF. Because of this effect a ring appears that becomes wider as more of the momentum is in the sideways direction. The Rings will close at higher ToF as the momentum points more and more away from the detector until the ring reduces to a dot again for particles with momentum pointing exactly away from the detector.

Figure 4: Simulations of the position spectra for increasing ToF windows. From left to right the ToF increases. A ring like structure is clearly visible

3 Experimental Setup

The experimental setup is comprised out of three main components. ECRIS, Electron Cyclotron Resonance Ion Source, this creates the projectile ions. CHEOPS, Charge exchange observed by particle spectroscopy, here interactions between projectile ions and gasses are studied. SirPhi, surface physics, which looks at interactions between projectile ions and surfaces. This part of the setup is not used in our experiment. The projectile ions from ECRIS are accelerated out of the ECRIS using an extraction field. This field multiplied by the charge of the particle determines the kinetic energy of the ion. The ions will than enter a 110° analysing magnet. This allows us to select a certain mass over charge ratio for the ions. This way we can ensure that only the correct ions are selected(other ions with the same mass overcharge should not be present or negligible). A retractable faraday cup is placed behind the magnet to allow for observation of the amount of selected ions. The faraday cup can be moved out of the way to allow the beam to continue to the other parts of the setup. After the analysing magnet the ions travel through vacuum tubes towards CHEOPS and SirPhi. A 45° degree bending magnet redirects the ion beam towards CHEOPS. Important for our experiment is the chopper just behind the entrance of CHEOPS. This chopper allows us to ”chop” the beam into short pulses. It does this by utilising rapidly switchable electric fields. Two parallel plates are placed above and below the path of the ions. An equal but opposite voltage is applied to the plates causing the ions to deflect towards the negatively charged plate. This leads to the ions missing the aperture further in the beamline. Rapidly switching the voltages on the plates will cause the beam to deflect towards the other electrode but this also means that the beam passed over the aperture. This allows us to ”chop” the beam into small bursts of ions.

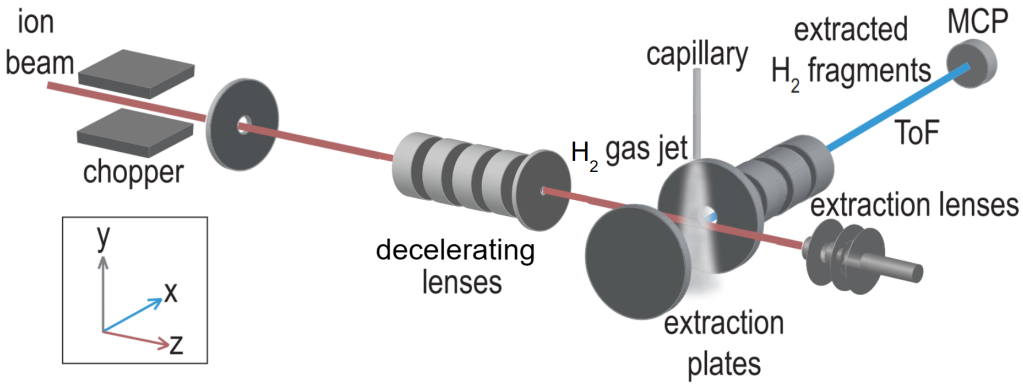

Figure 5: A schematic overview of the CHEOPS setup

The timer of the time-of-flight(ToF) measurements is linked to this chop thus allowing us to get consistent timing for our measurements. The entire setup also has various magnetic and electric focusing components to slightly redirect the ions along the beamline to improve the amount of ions that actually enter CHEOPS in a confined bundle. When transporting ions to CHEOPS we check with a faraday cup at the end of CHEOPS if they are being transported correctly. All the magnets are adjusted until the faraday cup shows a current that indicates a high amount of ions are hitting it.

3.1 Linear ToF setup

Previously the ToF part of CHEOPS consisted of a gas inlet letting in hydrogen gas and a parallel plate capacitor where one plate had a small hole in the middle. This hole would lead to a long flight

tube sticking out of the side with a detector (MCP) at the end. The beam would travel between the parallel plate capacitors and undergo electron capture due to the presence of hydrogen from the gas inlet. When suitable ions are used this could lead to double capture where both hydrogen ions will fly off in opposite directions. Hydrogen ions that traveled towards the hole could enter the flight tube and end up on the detector. The hydrogen ion moving directly away from the hole would be accelerated back towards the hole by the parallel plate capacitor to also get detected. These respective forward and backward ions could originate from the same original hydrogen molecule since double capture produces ions with opposite momenta. A lot of the Hydrogen atoms are not detected since the sideways emitted hydrogen will not travel through the hole and can thus not be detected.The interesting part here is the detour the backwards particle takes. This leads to a different time-of-flight for the forward and backward particle which can be used to determine the kinetic energy that the particles gain when double capture happens. The problem with this setup was that the long flight tube needed focusing elements to transport the hydrogen ions to the detector otherwise the amount of hydrogen that was detected was extremely low. These focusing elements will however destroy the pattern that the ions would make on the detector which could produce valuable data. For this reason a new detector setup was constructed.

3.2 Reaction Microscope setup

This setup has a longer acceleration region and is not made by parallel plates with a hole instead a lot of plates with larger holes are placed behind each other equidistantly. The plates are put on increasingly negative bias towards the detector to create the acceleration region. The flight tube is twice the distance of the acceleration region leading to a way shorter setup without the long flight tube. The flight tube is at the same potential as the last electrode plate of the acceleration region as to not cause a sudden deceleration. The setup still functions much in the same way as before. There is a part with an electric field to accelerate the hydrogen ions, a drift region without a field that increases the ToF and helps with time focusing and of course a gas inlet to introduce the hydrogen gas. The acceleration field has now become longer than it was before and the drift region or flight tube is shorter. The advantages are that the ions will be able to reach the detector without the use of focusing elements if the acceleration field is chosen correctly which will lead to an undisturbed position spectra on the detector, the spectra we are interested in.

3.2.1 Acceleration part

The acceleration region can be seen in the bottom part of fig. 6a it is comprised out of four threaded rods with insulating cylinder around it. Plates with four small holes to the sides and one big one in the middle are slid over the insulating cylinders with spacer ceramics in between. All spacers between the plates have the same length except for the bottom two plates. These plates are separated further to allow more space for the projectile ion beam since it will enter in between those two plates. The bottom electrode has a grid over the hole to ensure a homogeneous field near the bottom electrode. We can also observe that the bottom two plates have a notch taken out of them. This allows the projectile ions to pass through the plates instead of hitting them if for some reason they would have such a trajectory.

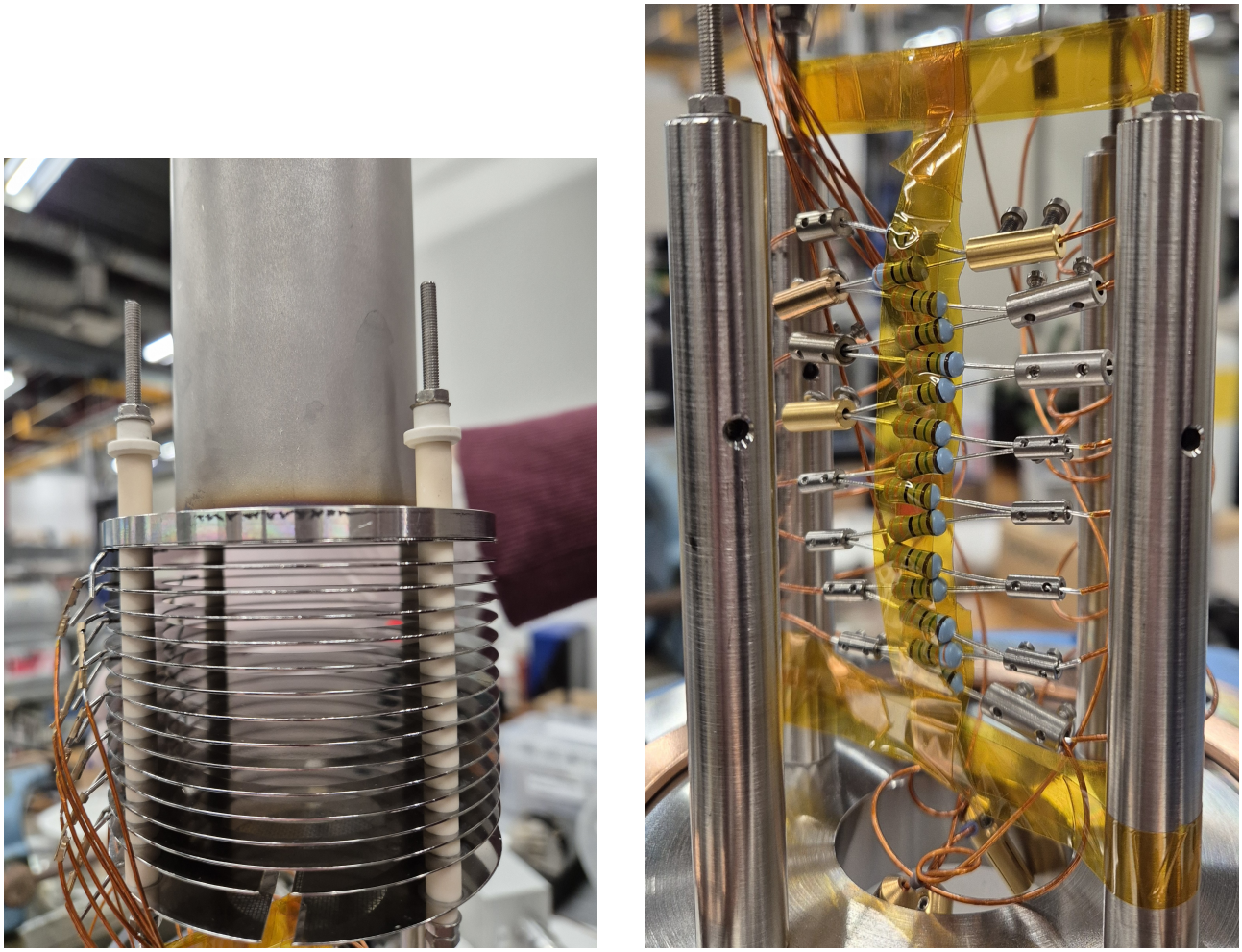

(a) (b)

Figure 6: (a) Acceleration plates and flight tube. (b) Holder of the acceleration plates and flight tube. These resistors in series hang in between the holder poles. The wires that go to the electrodes are attached by screw terminals as seen here. (The highest negative terminal is on the bottom right and the top left is ground)

Wire connections are made on the plates. These are used to apply a different bias to all the plates. The bottom electrode will get a positive potential and all the others a negative one. The positive potential will directly be applied to the plate. The negative potentials are supplied by one power source where identical resistors in series allow for a consistent voltage drop from plate to plate as seen in fig. 6b. The resistances are all 33.115 ± 0.045 MΩ. The voltage difference between the plates will be $\frac{V_{applied}}{15}$ except for the two bottom plates. Since they are exactly separated twice the distance but we still want a constant electric field they will have twice the ΔV. The bottom electrode will be $-\frac{V_{applied}}{15}$ and the second electrode will be $\frac{V_{applied}}{15}$ ($V_{applied}$ is negative and is the voltage applied to the resistor stack of figure 6b).

3.3 Detector

The detector consists out of two microchannel plates(MCP) and a delay line detector (DLD). The microchannel plates are there because it is difficult to detect single particles. This is the case because

if the ions will hit the detector directly it could only produce a few electrons which would be difficult to distinguish from noise and actually letting the ions hit the delay line could also be a problem as ions could all have very different energies and responses to electric fields. The MCP's will create an electron cascade that is measurable because a large cloud of electrons is created. The DLD allows us to detect the position where the ion hits the MCP.

3.3.1 Micro Channel Plates (MCP)

Micro Channel Plates are slabs of thin resistive material with a thickness in the mm range. These resistive plates have small bundles of capillary's through them from one face to the other. These tubes are at a small angle to the surface normal. When an ion, electron or photon enters a capillary it will hit the side. The side will than emit electrons via secondary emission. The electrons will in there turn also hit the sides and therefore create a cascade of electrons that will exit the MCP at the other end of the capillary. A bias is applied to the top and bottom of the plate such that the electrons will flow in one direction and to recharge the MCP after a cascade. The adventage of an MCP compared to other electron multipliers is the position sensitive nature of an MCP. The electron cloud position corresponds with the position of the incident particle. The Micro channel plate we use is a MCP stack. Which are two MCP's with opposite capilarry angles on top of one another. This leads to increased gain of the signal. The MCP can not only be used as an amplification device but also as somewhat of a detector. Once the MCP discharges the voltage will shortly drop. This can be used as a timing signal. The MCP used can be seen in figure 7.

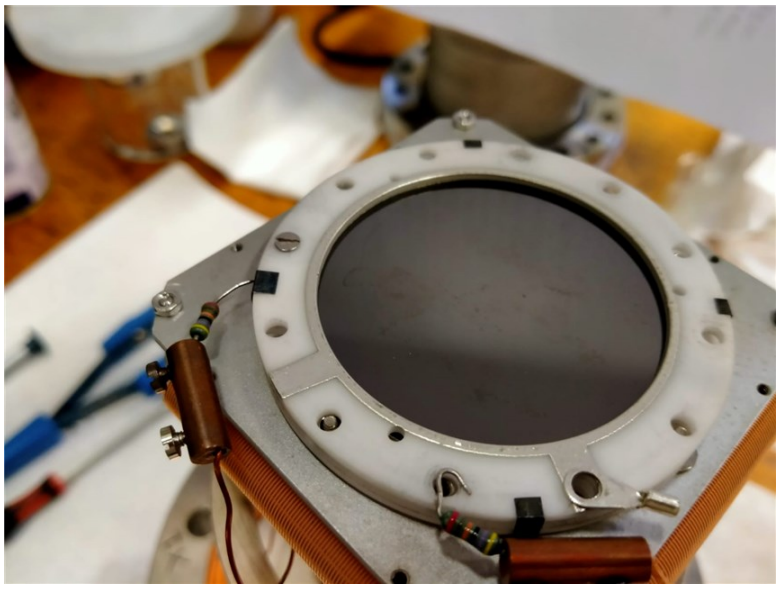

Figure 7: The MCP. The capillaries are not visible because they are very thin

3.3.2 Delay Line Detector (DLD)

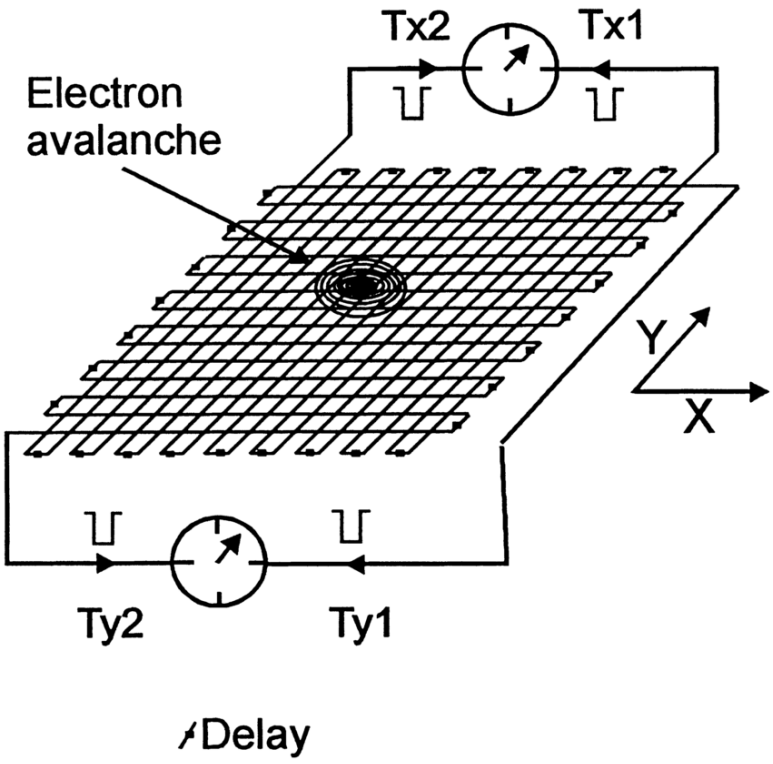

Figure 8: Schematic DLD. Take note of how the axis are defined [5]

The DLD is placed behind the MCP and is able to detect the electron cascade caused by it. This can be used to determine where the ion hit the MCP. The DLD consists out of two shaped wires as can be seen in figure 8 The ends of the wires are indirectly connected via a high voltage decoupling circuit to read out electronics. let's first consider one of the axis, the x-axis. The wire has two signal detectors, x1 and x2. When an electron avalanche hits the wire, a pulse will travel in both directions of the wire. The total time a pulse will need to travel from one end of the wire to the other is constant. This also means that

$$t_{totx} = t_{x1} + t_{x2}$$

Where t_{x1} and t_{x2} are the time the pulse takes to travel to x1 and x2 respectively. The timer starts when a signal is received from the MCP. There will be some time needed for the electrons to actually hit the wire (t_{travel}) and than some additional time for the pulse to reach the ends of the wire (t_{x1} and t_{x2}. The time difference between t_{x1} and t_{x2} will give us information about where on the x-axis the cascade arrived. The shape of the wire allows the cascade of electrons to hit the x-wire multiple times as seen in figure 8. The pulse that will now travel over the wire is an addition of the pulses for all the different wire pieces. This adds to one single pulse that is used for the position detection.
Where

$$\Delta t_x = t_{x1} - t_{x2}$$

The Δt_x will now be used to determine the position on the detector. The time that a signal takes to travel 1mm in the x direction is called the wire pitch. We can divide the Δt_x by twice the wire pitch to find the position on the detector. This exact same reasoning of course also works for the y-axis.

The next paragraph will highlight a problem that can occur with data acquisition due to the way hits are handled. A single particle will produce pulses on the delay lines which will travel over the delay lines towards the electronics and produce a t_{totx} and a t_{toty} that is consistent with all other particles.
Let's now think of a hypothetical situation where not just one particle but two particles hit the detector. let's also assume for simplicity that one particle hits the detector on the left side and the other hits the detector on the right side at the same time. These particles both produce a t_{x1} and t_{x2} but the order on which the are received on the electronics will be scrambled. It than follows that

$$t_{x1_{right}} + t_{x2_{left}} \neq t_{totx}$$

The measurement will than not be considered a real particle. This is an unfortunate effect of the setup since we would like to measure particles that arrive on opposite sides of the detector with little time in between. It could thus be smart to add some different logic to this system where if the MCP triggers multiple times and incorrect t_{totx} are found a salvaging procedure is preformed. This procedure would simply be adding the measured t_{x1}'s and t_{x2}'s until a correct sum is found.
The DLD, MCP stack and all read out equipment are provided by Roentdek and their manual was used to create the detector setup. Some of the specifics in how everything functions are not well explained in the manual and are also not easy to find.

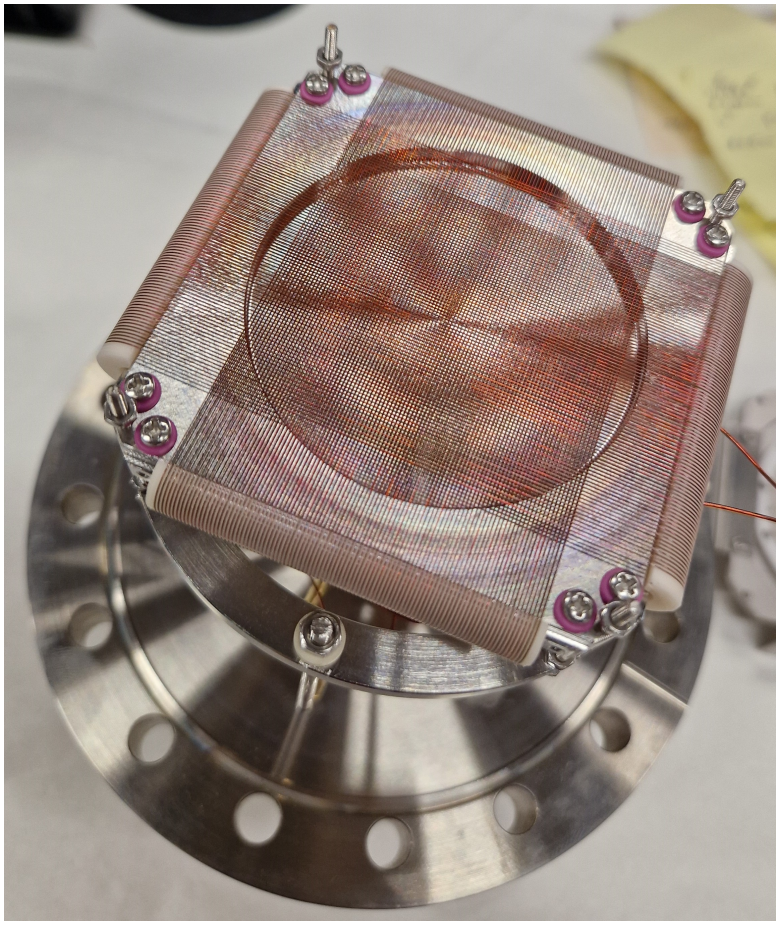

Figure 9: DLD with MCP stack removed from the top

The detector can be biased in different ways. For detecting ions it is recommended to use Roentdek's ion detection mode. However we chose to not use these exact voltages. Since our flight tube is very

	Ion detection mode (V)
MCP front	-2400
MCP back	0
Delay line anode Holder	0
Reference wires	250
Signal wires	300

Table 1: Ion detection mode suggested by Roentdek

close to the MCP we did not want a sudden field change to effect the detected positions and time. We thus chose to set the MCP front to the same voltage as the flight tube which has a typical value of -1000 V and simply changed the other voltages such that the voltage differences match the ion detection mode of Roentdek. Table 1 shows the bias applied in Ion detection mode.

3.4 Signal processing

Signals from MCP front and x1, x2, y1, y2 are collected. The signals of the delay line anodes might be somehow affected by the reference wires to reduce noise for example but this is not certain as explained before. All the signals are handled separately but undergo the same process except for the MCP front signal which is slightly different as will be explained later. The first thing that is done is amplifying the signal. This is done because further electronics are designed for signals of certain ranges(-2 V to 50 mV)[6]. After being amplified the signal will enter a Constant Fraction Discriminator(CFD). A CFD is used to turn our initial noisy analog signal into a clean block pulse that can easily be turned into digital data.

3.4.1 Constant Fraction Descriminator(CFD)

The CFD first converts a analog signal in a slightly different analog signal that is easier to work with. This process is shown in figure 10. The signal is first divided by a resistor-divider. This creates two pulses with different pulse heights. The Ration of the pulse heigths that we use is 0.35, Roentdek standard. The lower signal gets inverted and the high signal gets slightly delayed. The delay is done by an external cable inducing a delay of 2.25 ns, Then they are superimposed and create a bipolar signal as seen in figure 10.

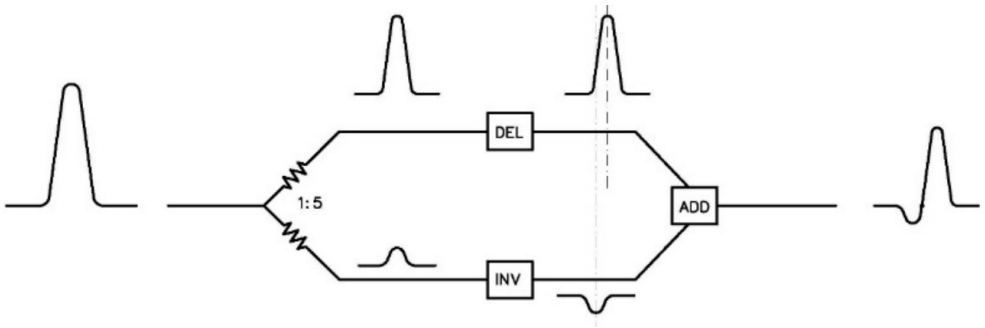

Figure 10: Schematic of analog CFD chain. left is the initial signal, right is the signal that allows for easier digitalisation[6]

This signal will now be used to produce a block pulse as seen in figure 11. Analog in shows the original pulse. The threshold is set such that it is close to the noise but only gets exceeded by an actual pulse. The leading edge trigger will give a high output when exceeding the trigger and will return to low when below the trigger. This could in principle already be used as the final signal to store the data but there is one problem with this method. The original signal does not always have the same height. If the original signal is very high the threshold will quickly be exceeded but if the signal is low it might only exceed the threshold near the peak of the signal. This will lead to a big time error. To prevent this time error the following is done. The analog signal from figure 10 is used in a walk comparator. This work similar to the threshold that produces the leading edge trigger. However this time the walk(threshold) is set to a level inside of the noise. The digital monitor in figure 11 shows that it will now trigger and un-trigger rapidly in the noise. As soon as the ”dip” in the signal comes in the digital monitor will turn to low. The walk is very close to the baseline value so as soon as the zero crossing happens the digital monitor will now be in the on state. This zero crossing is independent of the signal height due to the way the analog monitor signal is produced. An AND gate is now used on the leading edge trigger and digital monitor to obtain a singular block pulse that can easily be stored digitally and has timing independent of initial pulse height.

The threshold and amplification of the signal can be controlled for all the delay-line signals and the MCP front signal. The MCP front also allows us to change the walk level while this is preset for the delay-line signals. This difference lies in the electronics that do all the CFD steps. The MCP front signal travels through an amplifier (Roentdek FAMP1+) followed by the actual CFD(CFD1c). The delay-line signals go into ATR19-2b these allow two of the delay-line signals to be processed on one piece of hardware and contain all the CFD components. This leaves the MCP front with more adaptability than the delay-line signals. The electronics are a standard set of electronics provided by roentdek called the FEE2 set. It does not specifically mention why the CFD is different but Roentdek makes clear that MCPs can exibit vastly different characteristics from one to the other and also disclaims that MCPs should be thought of as consumable and will degrade over time even in proper usage. It is highly likely that the MCP signal simply varies to much between MCPs that extra control of the parameters is needed.

The callibration process is another important task in using these electronics. Roentdek gives instructions with images of how signals should roughly look and some common deviations from that signal and how to help alleviate some of these problems. Our signals did look similar to Roentdek’s images but we believe they are probably still far from optimal. There where also some patterns found in the digital monitor where an additional peak could be seen a fairly constant time from the first peak we unfortunately do not have pictures of these signals. This could indicate some reflected signals or it could also be accidental re-triggers of the MCP as it is charging back up after a discharge. This re-triggering behaviour will be discussed further later on in this report.

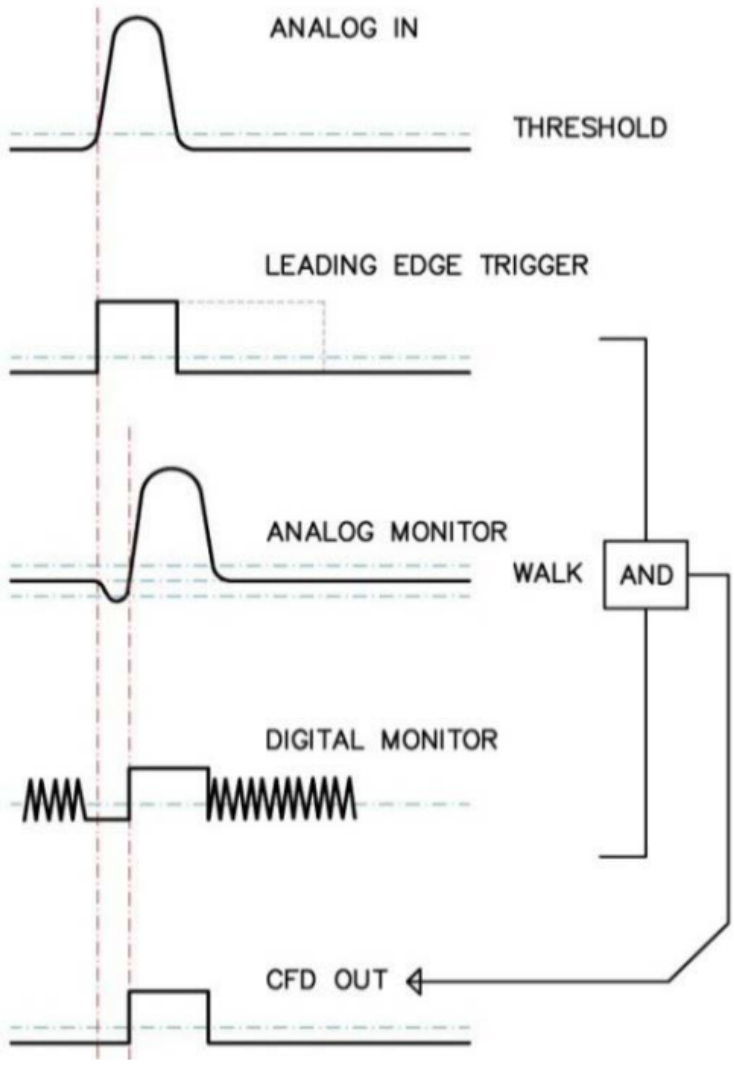

Figure 11: Schematic of analog to digital CFD conversion. Showing various steps in the process of digitalisation[6]

4 Results and Discussion

The results discussed are some of the first data taken with the new set-up(reaction microscope****) and some new data taken with the new detector on the old setup(small acceleration region, long flight tube and small hole for hydrogen to pass through towards the detector). The old set-up data we will discuss is from Ar^{6+} with 60 keV kinetic energy. The ions used to take data on the new set-up where Sn^{6+} 48 keV and He^{2+} 40 keV. There are some other important distinctions between the old and the new set-up that should be mentioned. The old set-up also had some erroneous voltages applied to the detector. This happened because we did not realise that we had a specially constructed detector (FT12TPz) where only a voltage had to be supplied to the MCP front and signal inputs, a voltage divider board would distribute the voltages correctly for correct operation. Since we did not realise this we did apply voltages to the other inputs. We are unsure how that was handled in the device but we did not find any unexpected results when voltages where applied to the components. We can conclude that it seemed to work at the time of the erroneous connection and it still seems to work. The old set-up also had a grid in front of the MCP which was removed when we switched to the new set-up. Another important distinction is that Ar^{6+} used the standard ion detection mode voltages on the detector while Sn^{6+} and $He^{2}+$ used a scaled variant as discussed before in section 3.3.2

4.1 Calibration

We will first discuss some of the plots that Roentdek supplies to check for a correct calibration of the electronics. It should be noted that Roentdek is not very clear about how exactly most of the functions work. The first type we will discuss is the consistency indicator which can be seen in figure 12.

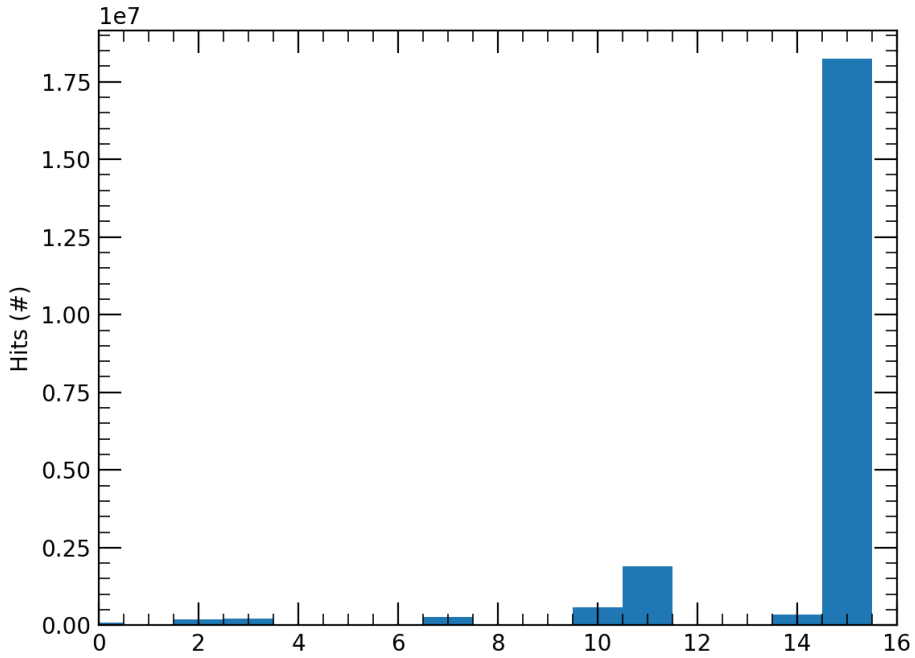

Figure 12: Consistency indicator graph for Ar^{6+}. 15 means that all the signal receivers received a signal while all other values mean one or more signal receiver did not receive a signal.

The numbers on the x-axis (consistency code) correspond to different TDC's registering a hit by the

following formula

$$Consistency = \sum k2^c$$

Where $c =$ a number corresponding with one of the TDC's of the delay lines from 0 to 3. $k = 1$ if the TDC registerd a hit and $k = 0$ if it did not register one. The window to receive a hit is started by the MCP signal and continues for a set measurement time. Thus 15 means that all the the delay line signal receivers obtained a hit. The signal shown here is thus a fairly good signal as it contains a lot of 15 and not very notable other peaks. Roentdek does not mention explicitly that measurement starts at and MCP signal but that seems the only way this plot makes sense otherwise the c should go to 4 and the axis should continue to 31 to take the mcp signal in mind. If it would measure from the trigger than the 0 code should also have a sizable peak for chops that produced zero measured charge exchange.

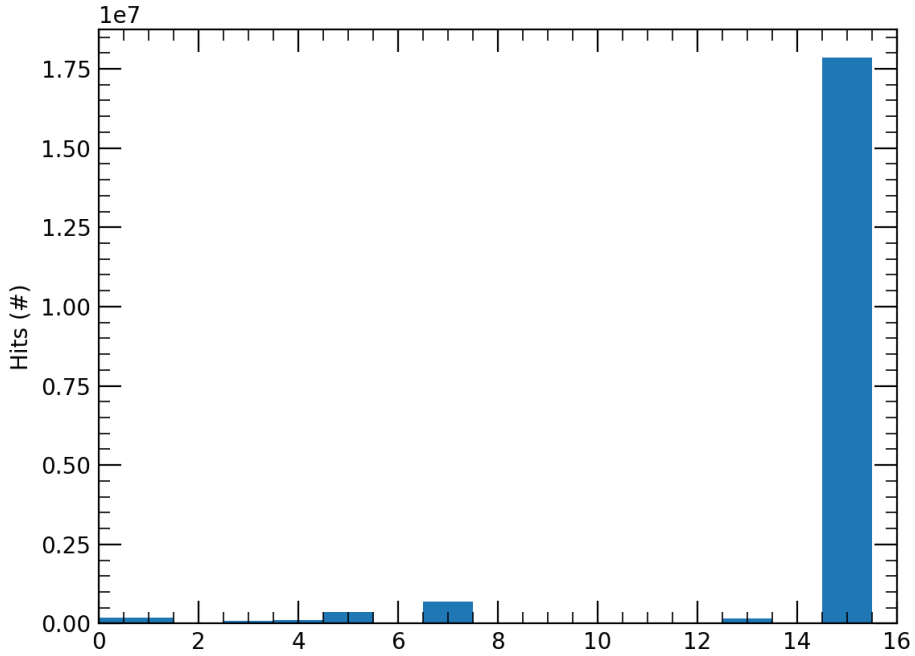

Figure 13: Consistency indicator graph for Sn^{6+}. 15 means that all the signal receivers received a signal and all other values mean one or more signal receiver did not receive a signal.

The consistency looks similar for the other cases as can be seen in figure 13 for Sn^{6+} which looks similar to the not shown He^{2+} case.

There is another important graph that Roentdek provides for calibration purposes. These are the sum u and sum v. They indicate the time sum of the x and y delay lines respectively. They plot how often a specific t_{tot} appears when a signal is received.

$$t_{totx} = (t_{x1} - t_{MCP)} + (t_{x2} - t_{MCP}) + C_x$$

$$t_{toty} = (t_{y1} - t_{MCP}) + (t_{y2} - t_{MCP}) + C_y$$

Where the t_{MCP} terms are present since timing goes with respect to the MCP hit. The C constants are set such that the t_{tot} peak is located at 0. If the spectra does not show only one peak but also peaks before the main peak this often indicates a pre-trigger problem. This means the CFD's of the delay lines are not set-up correctly causing it to trigger prematurely. Its not advised to set a narrow t_{tot} software window since these pre-triggers could be tied to a specific region on the MCP or Delay line detector. Setting a software window would than still produce artifacts on the spectrum. The better option is to change the CFD parameters. The sums for Ar^{6+} is shown in 14

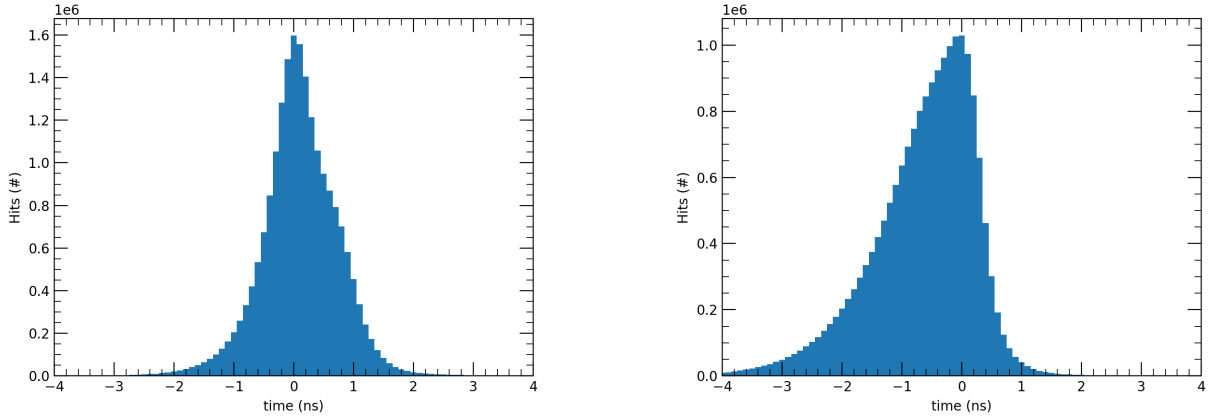

(a) Sum u. The time sum of the x delay line layer

(b) Sum v. The time sum of the y delay line layer

Figure 14: Ar^{6+} sum graphs. They do not show clear pre triggering

The spectra of Ar 6+ sum u in figure 14a shows no unexpected effects. The only notable feature is a slight bump in the spectra to the right. Effects that increase the t_{tot} are not discussed by Roentdek. One explanation could be that the big peak is actually a consistent pre-trigger and the slight bump is the correct signal, the distance between these peaks is often more in the range of 2 ns so it seems unlikely. It might be some other unknown effect. Anyway the effect is small and the spectrum indicates good functionality. The sum v in figure 14b shows an unexpected effect at lower t. The spectra to the left of the peak is unexpected and does not seem to be caused by pre-triggers since this does most of the time give a clear second peak. It could possible be caused by the erroneous wiring or some other effect. It is not very a major problem since much has changed since this measurement so further research into it does not seem needed.

The spectra for Sn^{6+} seen in figure 15 do show clear signs of pre-triggering. At the time we decided to start measurements with the current CFD settings because the time left was limited. We can clearly observe pre-triggers here and before making further data sets this should be fixed. The reason we have pre-tiggers for the new set-up is likely the case because of the different voltages applied compared to Ar^{6+}, the erroneous connections or a mix of both. This might influence the signals received by the CFD's.

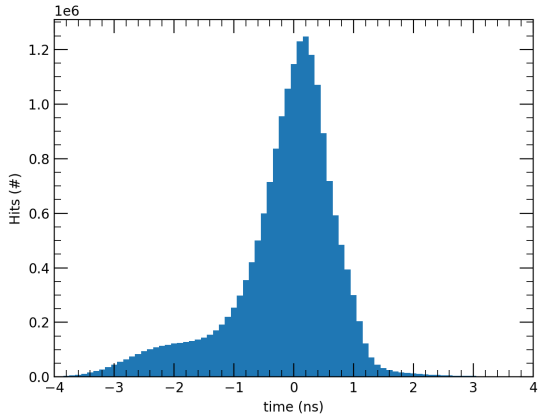

(a) Sum u. The time sum of the x delay line layer

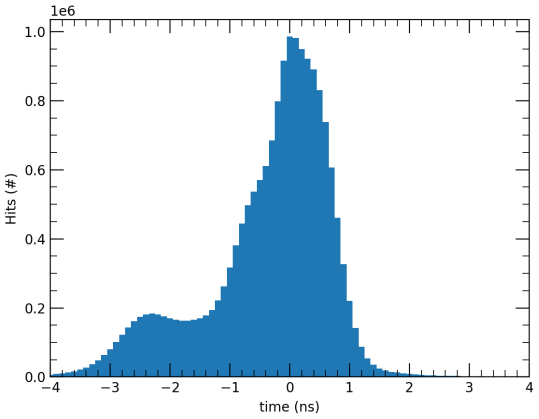

(b) Sum v. The time sum of the y delay line layer

Figure 15: Sn^{6+} sum graphs. They show pre triggering

Both sum u and v seem very similar and have similar width of the main peak. The pre-triggers do not necessarily seem to be tied to an artifact. The artifacts often look like smears over a part of the detector. It could be possible that the bright corner areas we will encounter later in the position spectra are caused by this. It is probably best to just take new data without the pre-triggers instead of somehow trying to salvage this data.

The sum spectra of He^{2+} is similar to the Sn^{6+} sum spectra. Therefore its likely it was not some fluke for the Sn^{6+} case and the CFD's should definitely be recalibrated.

4.2 Ar 6+

The ToF time is the time between the chopper signal and the MCP front being hit by an ion. The spectra for Ar^{6+} can be seen in figure 16

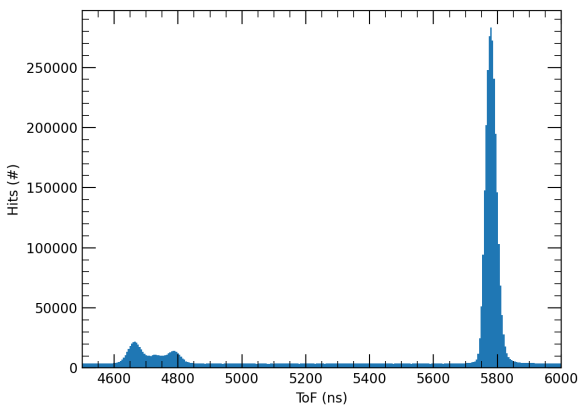

(a) Zoomed out. Showing H^+ peaks on the left and H_2^+ peak on the right

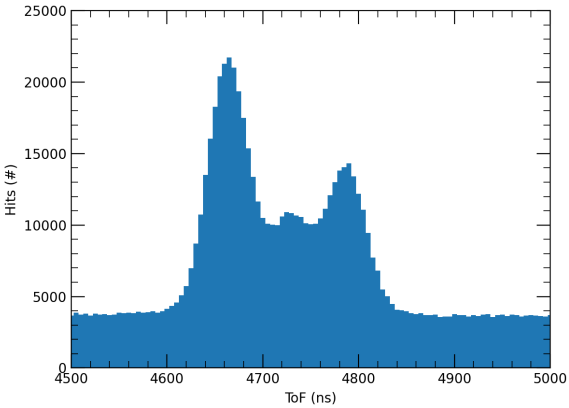

(b) Zoomed on H^+ peaks. from left to right: forward, 0 eV and backward

Figure 16: Ar^{6+} Time of Flight

The ToF looks as expected. Previous measurements of the ToF had already been done with the old detector without delay lines and they look similar to this as can be seen in[1]. The time difference between the forward and backward peaks corresponds to the expected value of about 150 ns. The spectrum shows forward emitted protons, 0 eV emitted protons and backwards emitted protons. These distinguishable peaks arise due to the small hole in the detector plates of the old set-up as explained in section 3.1.

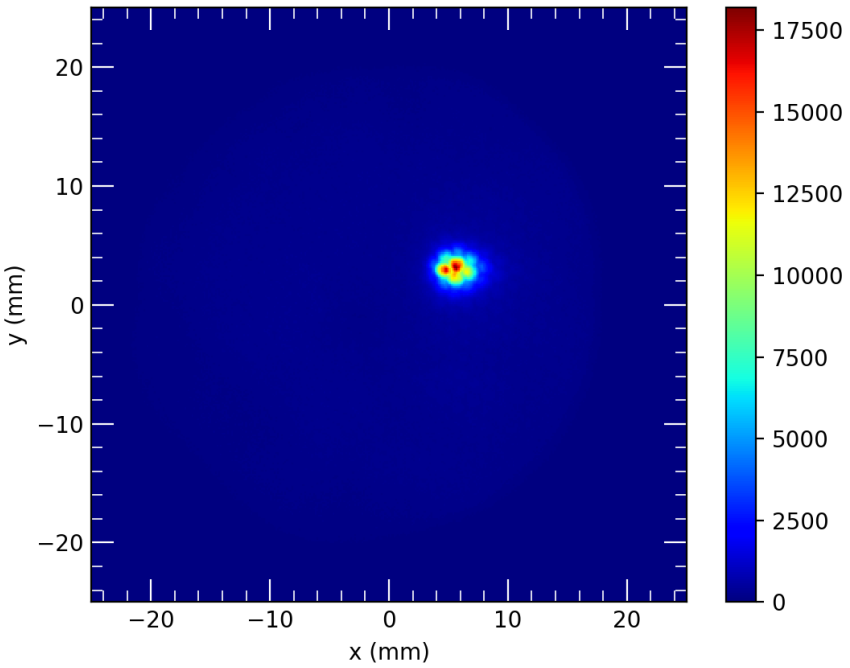

Figure 17: Position spectra of Ar^{6+}

The position spectra of Ar^{6+} can be seen in figure 17. To create this small focus on the detector the voltage on the focusing electronics where slightly changed. The idea being that a good focus would also mean most of the ions would end up on the detector. The spectra shows that the focus is not in the middle of the detector. We tried to get the focus more towards the middle but to no avail. This might mean the old setup had a slight misalignment in the parallel plate capacitor or focusing electronics or it could also be the case that the earth magnetic field might cause this. If we where to use an estimation we could use the following formula

$$F = q(v \times B)$$

$$F = ma$$

$$d = \frac{1}{2}at^2$$

combining the equations lead to

$$d = \frac{1}{2}\frac{q(v \times B)}{m}t^2$$

Where d is the deflection.
Since the old flight tube faced roughly towards east we can take the cross product as a simple multiplication resulting in a deflection of the ions upwards. Realise that the ToF given here is time of chop till time of detection so not the actual flight time of the protons. From figure 16a we can determine that the flight time of H_2^+ to be approximately 2200 ns. We know this because H_2^+ has the same kinetic energy as 0 eV H^+ but has double the mass. This means H_2^+ has half the velocity and will thus take twice the amount of time to reach the detector. The ToF difference between 0 eV H^+ and H_2^+ is 1100 ns thus H_2^+ actual flight time is 2200 ns. Assuming a strong earth magnetic field of $65\mu T$. Now using that the flight tube is 2 meters we find that the deflection is 7 mm which is similar but slightly smaller than the displacement from detector center we see in figure 17. Meaning that the earths magnetic field is likely at least a contributor in this off centering. I also assumed here that earth magnetic field is completely following the earths surface which is not the case in The Netherlands. meaning that the deflection upwards due to the magnetic field is probably considerable lower.

The next spectra we will look at are not spectra produced by Roendek's cobold but are produced by an under development software cabouter by Emiel de Wit. This software allows us to scroll through the ToF spectra and receive the corresponding position spectra. The position spectra seen in figure 17 used data from all the flight times but cabouter allows us to select a part of the flight times to view in a position spectra. This allows for much greater insight in the data.

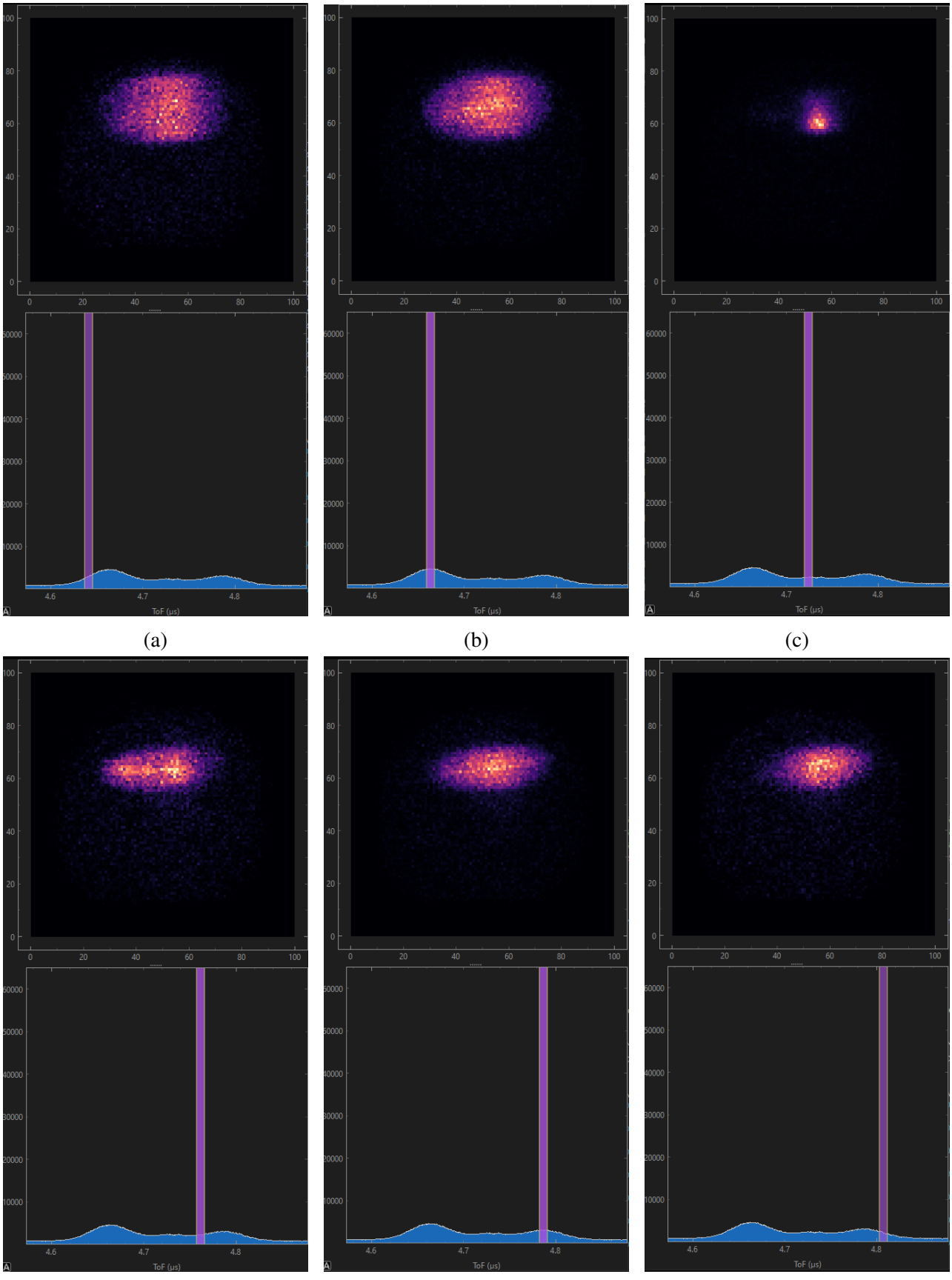

(a) (b) (c)

(d) (e) (f)

Figure 18: (part 1) Position spectra of Ar^{6+} for ToF windows. The ToF increases for every figure. The actual ToF window is shown below the position spectra

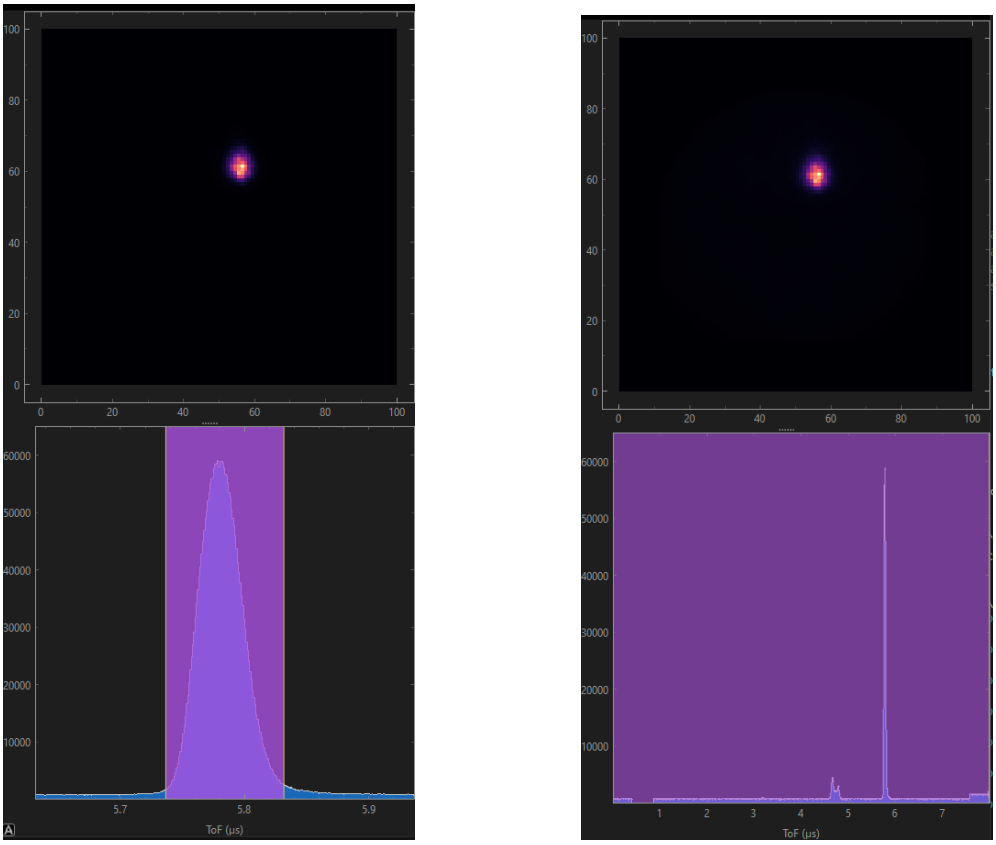

(a) (b)

Figure 19: (part 2) Position spectra of Ar^{6+} for ToF windows. The ToF increases for every figure. The actual ToF window is shown below the position spectra

First of all we should appreciate how this method of looking at the data reveals way more information than the spectra before. Not only does the extremely intense H_2^+ peak not dominate the spectra at other selected ToF's, it also shows us information per peak or section of the ToF spectra.

We can tell from figure 18a and 18b that the forward H^+ peak completely hits the detector since there is no intensity on the sides of the detector. We can also observe a slight switch of position as we increase the ToF it moves slightly upwards. A similar effect is observed for the backwards peak. Figure 18d, 18e and 18f show the backwards H^+ peak. Again the peak is confined on the detector and is again moving a bit as we increase the ToF. It moves more towards the right instead of up, which is unexpected since we would imagine that a shift in position would arise from a shift in interaction region of the ion beam with the hydrogen gas. If this was the reason for the shift we expect them both to move the same direction. Another observation is the 0 eV H^+ peak in figure 18c has a similar focus point and focus as the H_2^+ peak in figure 19a. This is as expected from a particle with the same charge, half the mass and double the velocity.
Another small note is that the data to make these plots still came from Cobold since the data acquisition of Cabouter is still a work in progress. We can see at low ToF and high ToF in figure 19b some data handling problems of Cobold. When data is loaded again in cobold it seems that part of the low ToF spectra vanishes and some high ToF gets extra hits as can be seen in the figure. It is probably a problem with Cobald loading in data. It seems like the missing data might be added to the high ToF data. Why this happens is unknown. It is another reason to switch data acquisition to other software.

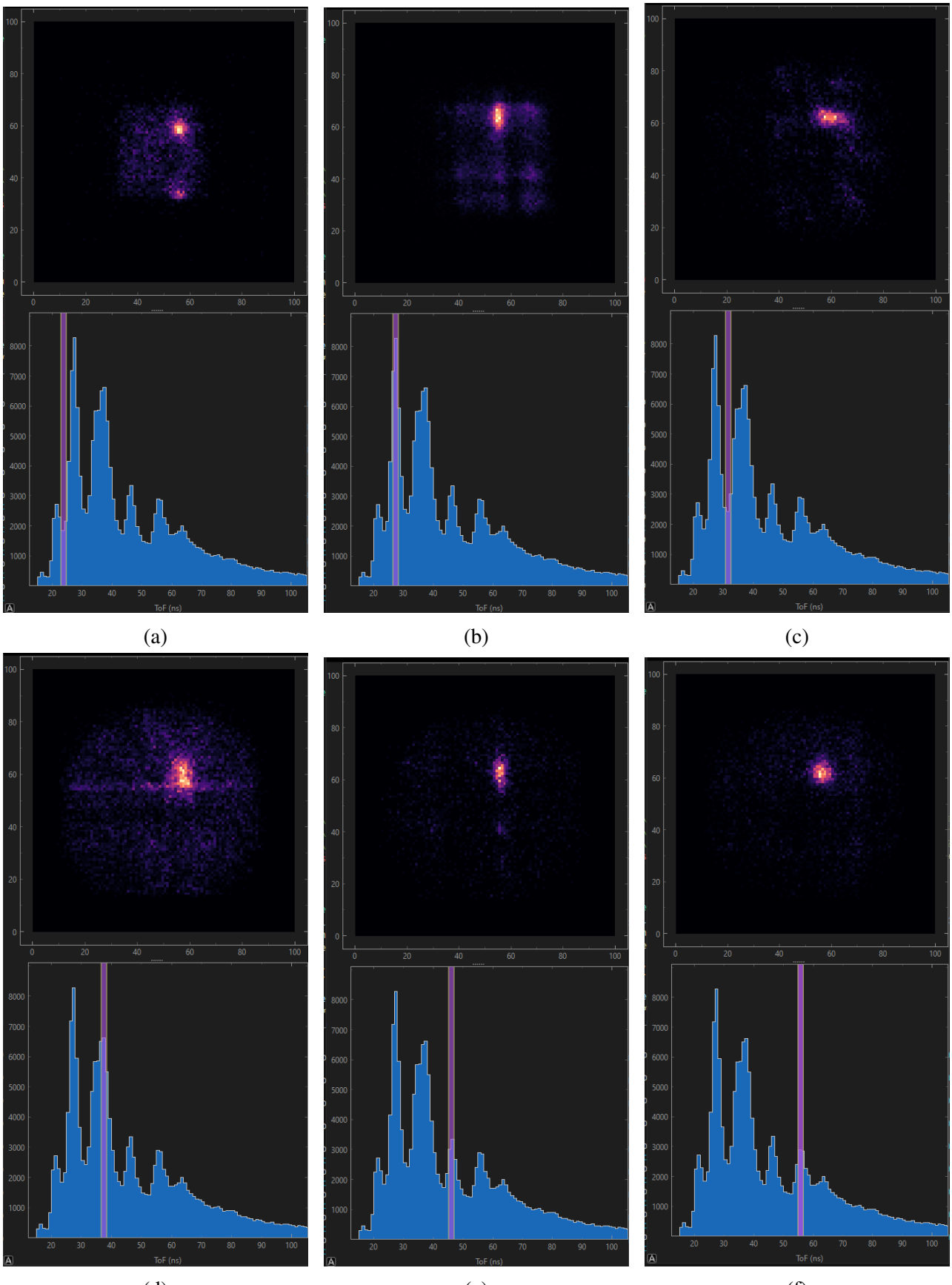

(a) (b) (c)

(d) (e) (f)

Figure 20: (part 1) Position spectra of Ar^{6+} for Dt windows. The Dt increases for every figure. The actual ToF window is shown below the position spectra

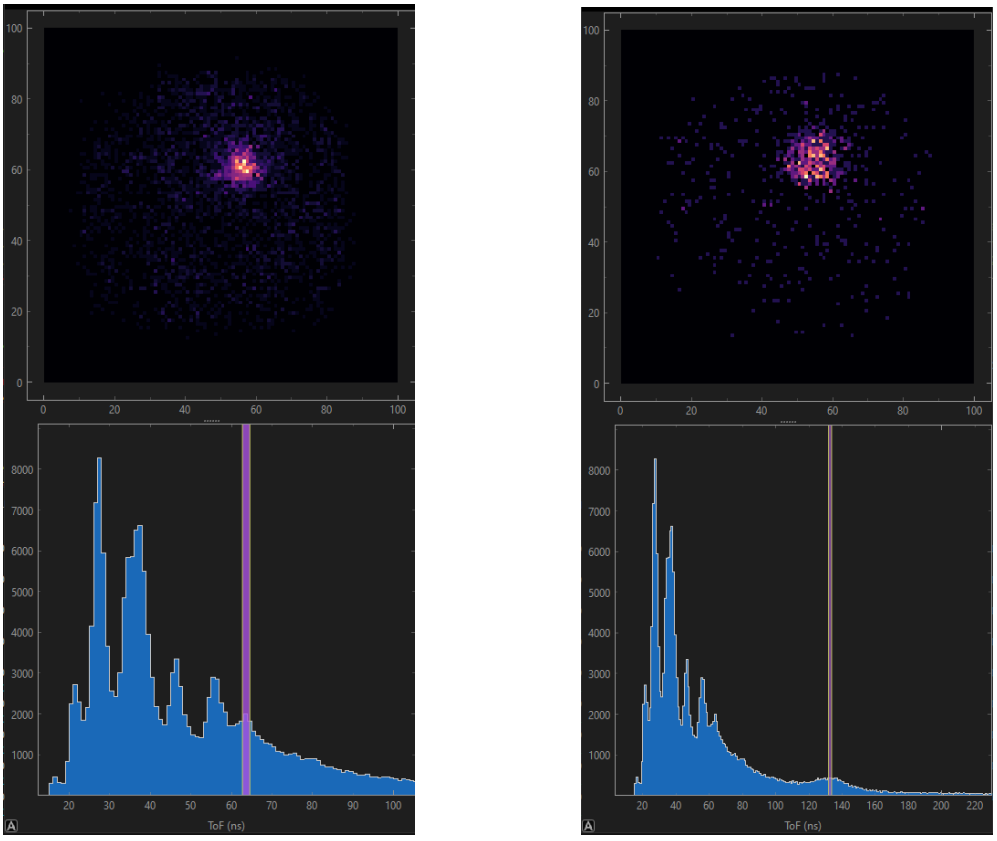

(a) (b)

Figure 21: (part 2) Position spectra of Ar^{6+} for Dt windows. The Dt increases for every figure. The actual ToF window is shown below the position spectra

Figures 20 and 21 show a different bottom graph than before. Instead of ToF is it now the difference in ToF between subsequent hits. I will explain this further. The measurements works by chopping the beam and starting the measurements. For some time the detectors will now measure when and where ions (or noise) arrive on the detector. All the ions that hit the detector in one chop are grouped together. What this graph shows is the time between these subsequent hits in bins and where these subsequent ions hit the detector is shown above it.

If we look at figure 20 in alphabetic order we increase the time after a initial hit. We can observe a bit of a pattern form at the low Dt. Roentdek also recommends that the dead time is always taken as 25 ns but the weird pattern seems to only disappear after 35 ns which could indicate that the MCP is not working correctly. The effect is still present with the new set-up where the correct voltages are applied as we will see in later figures. It could be that the MCP is simply spend. Roentdek does mention that MCP's should be seen as consumables and that at some point MCP's have to be replaced. The Dt spectra also shows peaks which are unexpected. It could be that these peaks and the weird spectra are somehow linked to the MCP's recharging where reflections give rise to periodic retriggers of the MCP causing these peaks and weird spectra. There is also an interesting peak at 130 ns Dt as can be seen in figure 21b. This peak corresponds with the backward H^+ peak. We can check this by observing the ToF distance between the forward and backward peaks in figure 16b which is around 130 ns just like the peak observed in figure 21b. Scrolling through the peak does not show the rings from the simulation unfortunately. This is also not expected since the set-up has a too long flight tube

and focusing electrodes that interfere with the position of the hydrogen ions on the detector. We could possible make the peak clearer by setting additional conditions on the Dt spectra. Creating a window of where the first hits will have to be in could be a useful. This way we can select the H^+ peak or the first part of the H^+ peak so we obtain less of the noise and uncorrelated triggers.

4.3 Reaction microscope consequences

In this section we will talk about the most noteworthy differences between the simulation of the reaction microscope and the reaction microscope in reality. We observe a stark difference between the interaction region assumed in the simulation and the actual interaction region. The interaction region was assumed to be a very precise location for the simulations but in reality the interaction region seems to span over at least the entire projectile ion pathway in the acceleration region. This will influence the spectra in such a way that the rings from the master thesis of Robbert Julius[2] will not be visible. We will thus use another method of determining the energy emitted from the double capture and other possible momenta that the hydrogen fragments could acquire. The method we will use is measurements in coincidence. Since when double capture occurs two hydrogen fragments will be created which can be detected. We can determine the time difference between these hits and the position difference which we can use to determine the kinetic energy that the fragments acquired during double capture. Our experiment uses small ion bunches thus the chance that an interaction takes place is not very high. If an interaction occurs with an ion bunch this is often only one interaction. We can thus use the difference of ion position and ToF in one chop to look into the fragment energy. In subsection 4.4 and 4.5 we will see how this is used exactly.

4.4 Sn^{6+} 48 keV

In this section Results for the projectile ion Sn^{6+} are discussed. The new setup is used for these measurements and an extraction electric field of $1.7 \cdot 10^4 V/m$ by applying a potential of 1000 V to the resistances that handle electrode voltages.

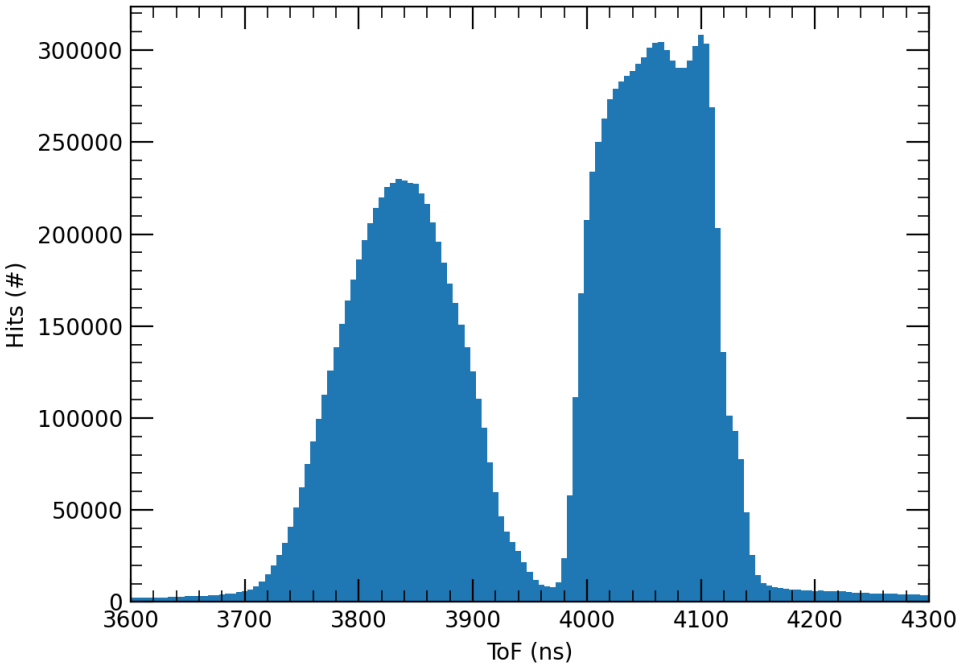

Figure 22: Time of flight spectra of hydrogen fragmets as a consequence of charge transfer with Sn^{6+}. The first peak belongs to H^+ and the second peak belongs to H_2^+

The position spectrum for Sn^{6+} is shown in figure 22. The H^+ peak is the peak on the left side. We do not see a forward and backwards peak that we did see for the linear setup in figure 16 but that is to be expected. The 2D setup does not utilise a small pinhole for the fragments to travel through and thus accepts all hydrogen fragment orientations. This leads to a singular H^+ peak. It also explains the size of the H^+ peak with respect to the H_2^+ peak. The peak is almost as big as the H_2^+ peak. This is the case because more of the H^+ is measured and does not get lost by hitting the extraction plates. This is not a completely fair comparison since different projectile ions are used but the size of the H^+ is generally way smaller than the size of the H_2^+ peaks for all previous experiments done on the linear setup. We also observe a clear H_2^+ peak although the shape of the peak is not entirely smooth. I will discuss the shape more under figure 24

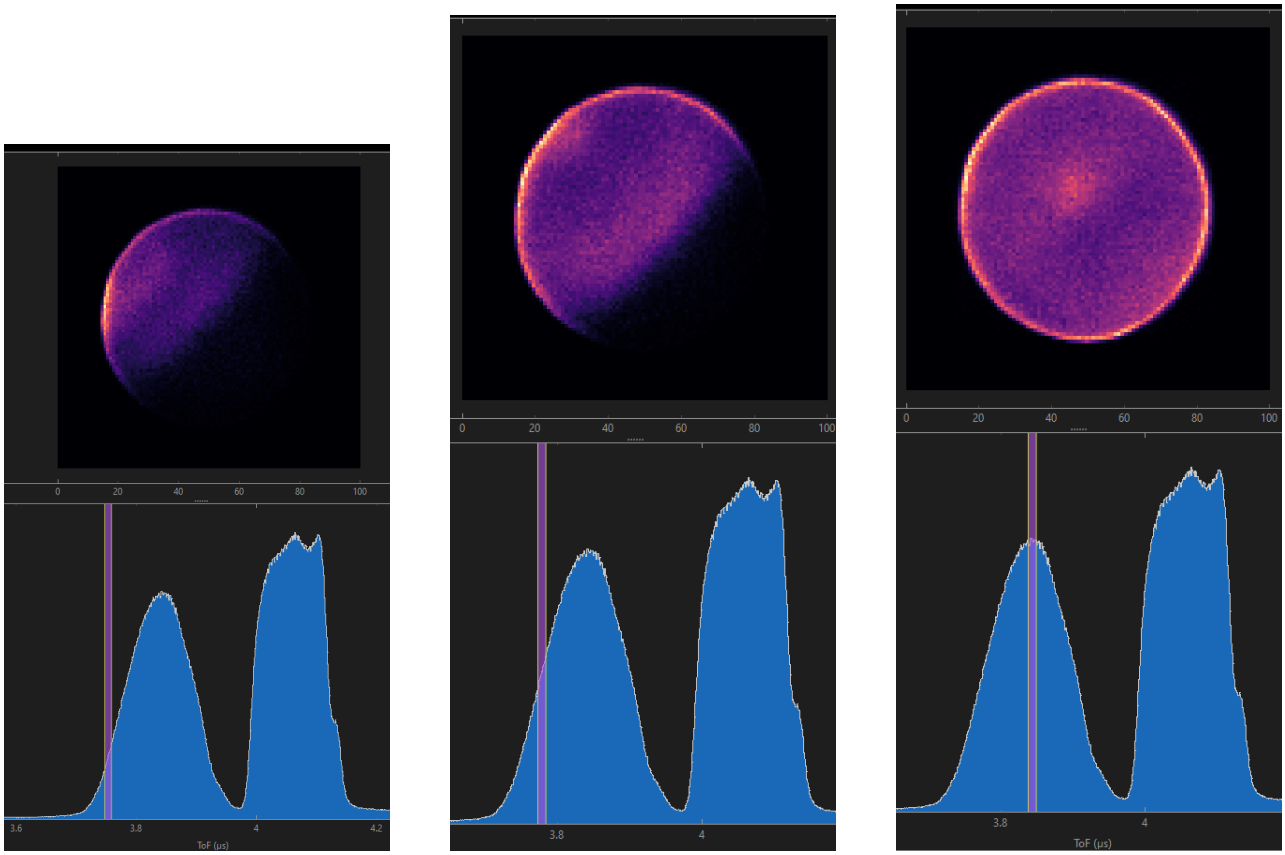

(a)

(b)

(c)

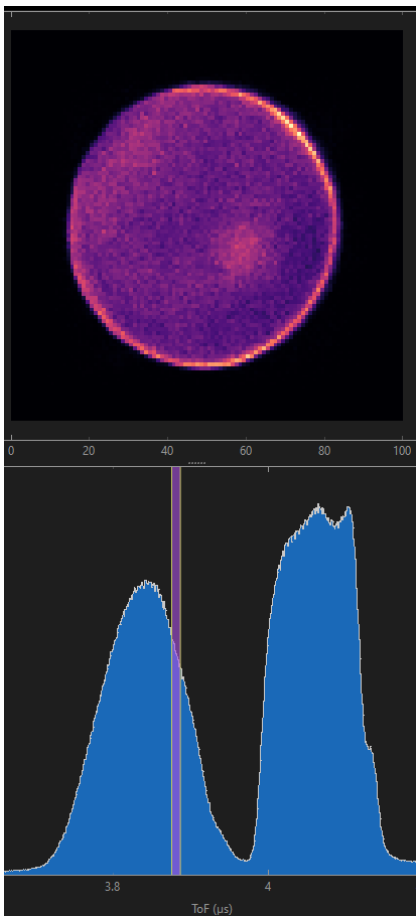

(d)

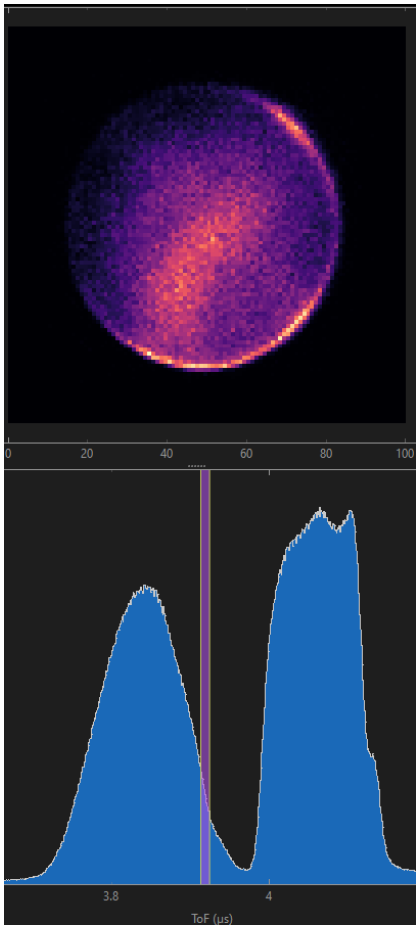

(e)

Figure 23: (part 1) Position spectra of Sn^{6+} for ToF windows of the H^+ peak. The ToF increases for every figure. The actual ToF window is shown below the position spectra

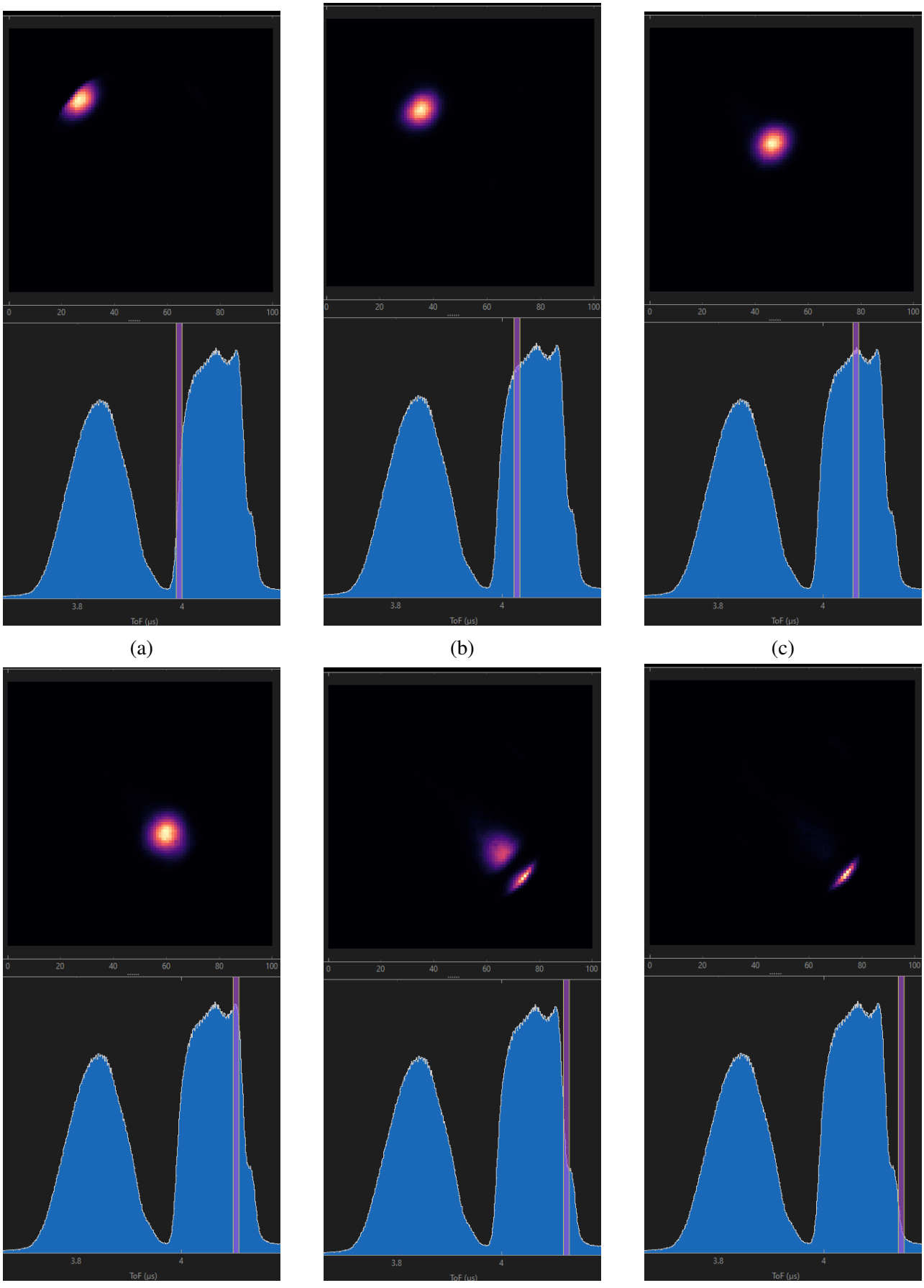

(a) (b) (c)

(d) (e) (f)

Figure 24: (part 2) Position spectra of Sn^{6+} for ToF windows of the H_2^+ peak. The ToF increases for every figure. The actual ToF window is shown below the position spectra

We can clearly see the effect of a long interaction region in figure 24. The H_2^+ which has 0 eV kinetic energy gets accelerated towards the detector by the electric field. The start of the H_2^+ peak seen in figure 24a shows that a bright spot is present in the top left of the detector. This thus means that hydrogen is detected here first. As we increase the ToF the peak shifts over towards the bottom right side of the detector. The peak shifting is due to the large interaction region. The hydrogen peak shifting position is a result of the projectile ions moving through this large interaction region. Hydrogen created closer to the chopper, entrance of the beam, will arrive at the detector earlier than the hydrogen created near the end of the electrode plates creating this shift.

There is another interesting effect visible at the end of the peak as can be seen in figures 24d, 24e and 24f. The peak is absent in a small region. We can also see in the ToF that before we go over this spot we get an additional peak, the highlighted area in figure 24d. There also is a bump in the ToF spectra just after this black spot. This suggest that some field is causing the hydrogen ions to deflect to the top left and bottom right side of the detector. It is not a dead spot on the detector as we can clearly see hits in that region in figure 23. This black spot not being present in figure 23 also means that this disturbance is likely not close to the detector. Since a disturbance close to the detector would likely also deflect all the H^+ with some sideways momentum away from that spot. Considering the shape of the electrode plates could also be helpful. The electrode plates have a thin part due to elongated notches near the entrance and exit of the ion beam as can be seen in figure 27. It could possibly be that this shape somehow has an influence on the spectra. We would however also expect a similar effect near the entrance(top left) because the electrode is the same shape over there. It could be that the target ions are already deflected towards the plates since they already traveled some distance through the electric field. Alternatively it could be that the start of the acceleration region is not captured on the detector meaning that the alignment of the acceleration region and detector is not optimal.

The black spot could just be due to passing over the thin part of the electrode followed by the notch allowing the hydrogen to pass through again. This would than mean that the alignment of the acceleration region is not straight onto the middle of the detector. This in itself is not a big problem but the problem is the field that the thin part of the electrode causes. In the ToF in figure 24 we can see the effect on the H_2^+ peak. The dip in the peak might be a result of the field of the thin electrode slowing down a portion of the hydrogen or alternatively the small peak behind the dip might be due to acceleration caused by the electrode. This is thus something that effects both the position spectra as well as the ToF spectra. However the effect for the coincidence might be small since this effect is mainly present near the edges. while most of the double capture near the edges will not give two hits because there is a high likelihood that one of the hydrogen ions will miss the detector when there is some momentum away from the middle of the detector. The sideways emitted hydrogen originating closer to the center can also get close to the side of the plates which might be another factor that leads to errors and a distorted coincidence.

looking into the the spectra observed in figure 23 we see a distribution of ions coming in from the top left and moves towards the bottom right. It is not a concentrated point as was the case for the H_2^+ peak in figure 24 because the ions have initial momentum leading to this distribution moving over the detector. This data might not be usable to determine the energy of the fragments like this but some data handling can change that.

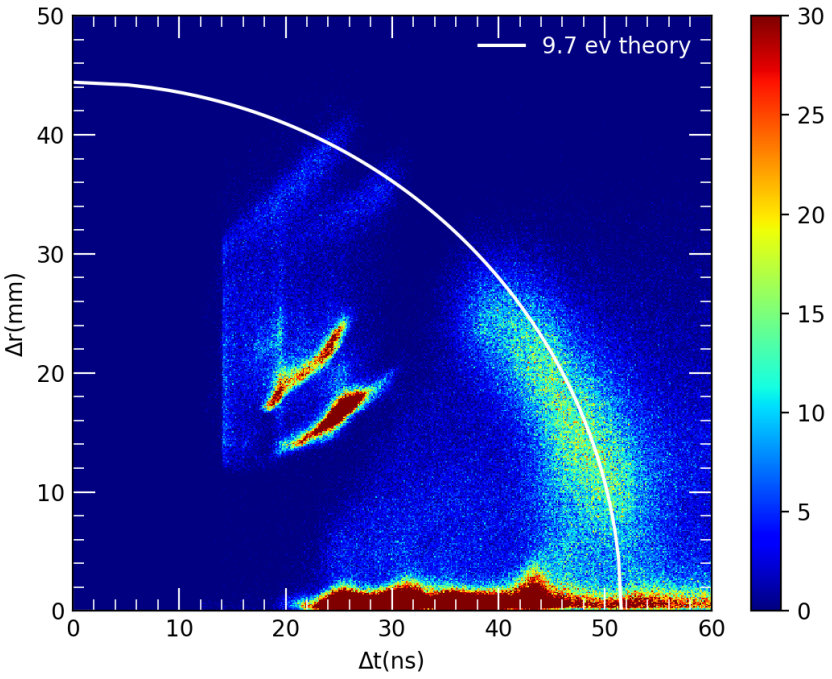

Figure 25: Coincidence of Sn^{6+}, Δt is the time between subsequent MCP hits in one group, Δr is the position difference on the delay lines between these same hits, The white line corresponds to what theory predicts, the colors corresponds to the amount of hits

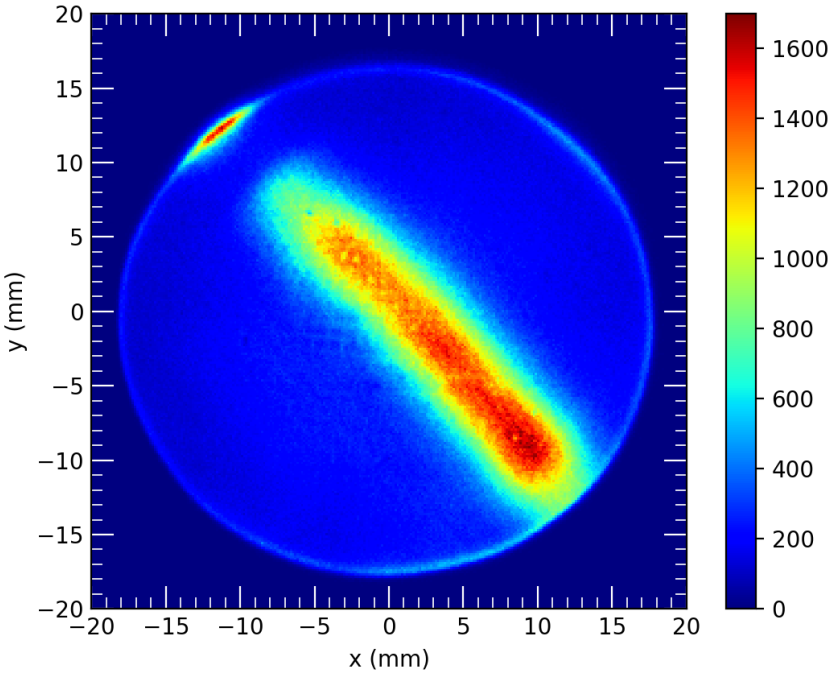

Figure 26: Position spectra of Sn^{6+}, The color corresponds to the hits on a specific position, this spectra shows all hits. Note: the spectra is flipped with respect to figure 24 due to data handling

The coincidence measurement can be seen in figure 25. The difference in position and time between the subsequent hits in a group are shown. The white line from theory uses equations 13 and 14 and varies $E_{\|}$. The figure shows that there are ions that broadly follow the line from theory which means the setup functions as envisioned. There are however a lot of other features present in the spectra which i will address now.

First of all the red spots. They are spots where a high amount of ions are located, so much so that the color scale would be so high that there was very little contrast around the white line thus the color scale was fixed to 30 hits per bin as a maximum. The location of the red region tells us something about our detector. The bottom red stripe around Δ r is most likely due to the MCP firing multiple times of a single ion. While doing measurements we observed that often when a hit was detected a second hit right after the set dead time would be registered without any explanation besides electronics. This happened independent of the ToF of the initial hit. We assume that this second hit is a consequence of the MCP accidentally firing again. It could be that this happens because the MCP has been stored in sub optimal(non vacuum) conditions for an extended period of time or MCP's might always suffer from this problem.

There is also a region around 20 ns with high intensity spots. It could be that these are due to the MCP recharging. Looking at figure 32 reveals that at low Δ t the hits follows a structured pattern which I think could be due to accidental discharges as the MCP is being recharged. We can not be sure but it might be wise to replace the MCP and see if these problems are still present than.

More interestingly let us now focus on the actual data. The data does not go beyond about 30 mm and 35 ns. This is not necessarily a dead time issue as can be seen in figure 40 where it disappears around 90 ns. So it seems to be tied to the distance between hits. It could be that somehow the fragments are deflected more towards the center but that would still produce ions with a lower Δ t most likely which we do not see. The sudden stop in the spectra might also hint at ions missing the detector. This is also likely if we consider the long interaction region. If most of the momentum is parallel to the detector and the origin of the fragments is not exactly in the middle there is a high likelihood of at least one of the fragments to miss. We do however expect that still some particles should hit the detector in those circumstances while we observe non. If we take into account that the theory does seem to match the present spectra well it might be that the detector active area diameter is only 30 mm. This should not be the case according to rountdek which states that the diameter should be closer to 43 mm. If we look at our position spectra in figure 26 we can see that it is also smaller than 43 mm diameter. It is closer to a 30 mm diameter. We previously thought that this was simply because the delay line time difference conversion to position data was not done properly yet. This would mean that the spectra would have to get stretched out. This would than in turn make our line from theory in figure 25 not align with the data anymore.

There are three options. It could be that cobold is slicing off a part of our spectra such that a smaller area of the detector is used. This seems unlikely since figure 26 seems to show some edge effects of the MCP on the detector(white lines on the edges) indicating that it is actually the edge. The second option is that the MCP is actually smaller than we think. This theory is also supported by the other theory that the blackspot on the detector is due to the notch in the electrode plate. we know that the inner diameter of the electrode is 36 mm, if we are able to see one of the notches so clearly close to the edge of the detector the other notch should also be present in the spectra if the MCP is 43 mm. It might be that the other notch causes the effect in the bottom right of figure 26 which would suggest

the MCP to be about 43 mm. If the MCP is actually smaller than expected than this should be fixed when the new MCP is installed since this one was delivered by roentdek as part of the detector. The third option is that the spectra should be stretched. We will than have to find the reason that the theory line has a different curve and position than the data.

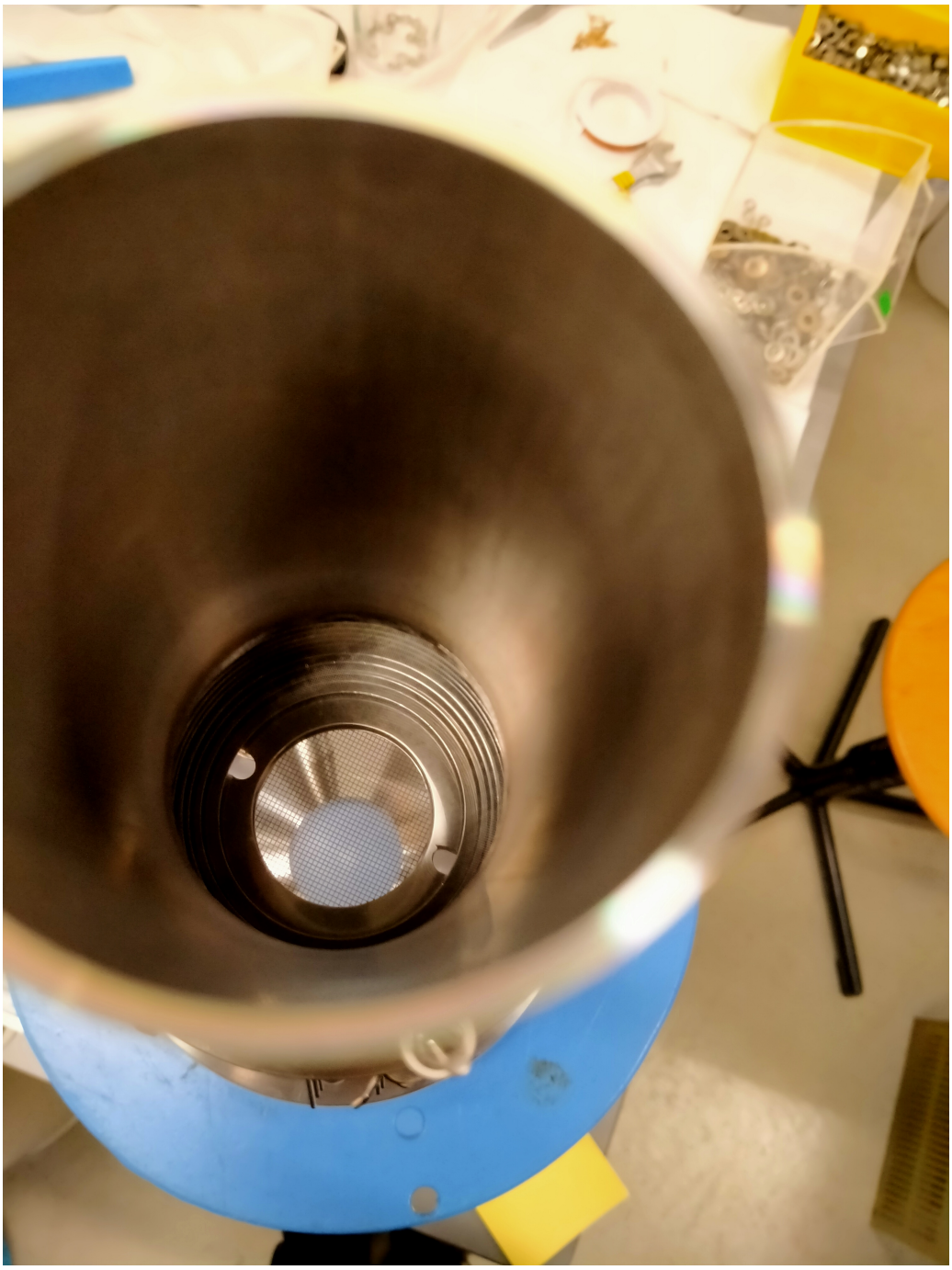

Figure 27: The acceleration region and flight tube. This is a view from the flight tube. This resembles the point of view of the detector. The notches are clearly visible.

Another feature to note is the low intensity from 2 mm to 8 mm around the theory line in figure 25. This is most likely due to an increased local dead time of the MCP. An MCP is generally more difficult

to trigger multiple times on the same capillary because it will locally be depleted of electrons[7]. The paper does not give insides into how locally exactly. It mentions that a single capillary will have to recharge for about 10^{-2} S but I imagine that not all the ions with low Δ r will actually use the same capillary. So we can not say for certain this is the problem unless we look more into the specifics of the MCP. It could also be that the backwards emitted hydrogen hits the grid on the last electrode or is lost after passing through the grid. Utilising equations 7, 9 and 8 we can calculate how far the particle travels backwards. The time is calculated by setting the derivative of equation 9 to 0. The particle travels a maximum of 0.55 mm backwards in our setup assuming 9.7 eV kinetic energy. Which is a very small displacement taking into account that the separation of the plates is 7.1 mm and we aligned the plates such that the ion beam passes through the middle. It thus seems unlikely that this is the problem.

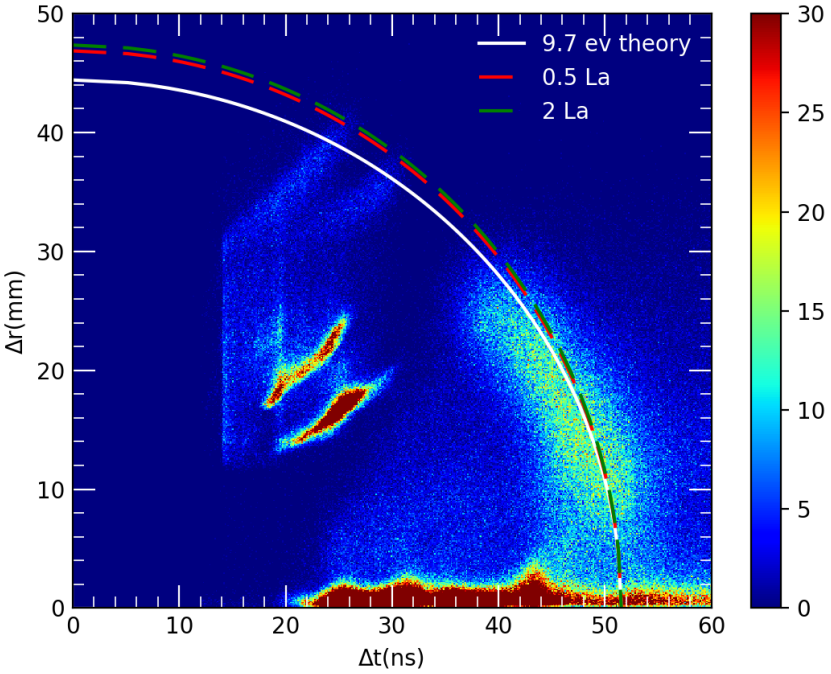

(a)

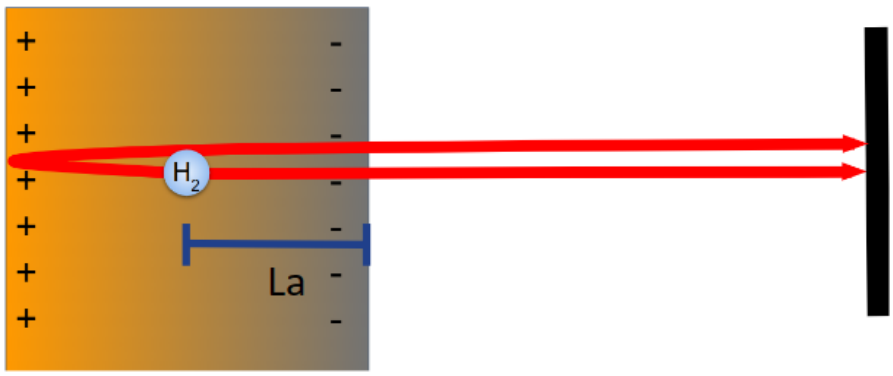

(b)

Figure 28: a) Coincidence of Sn^{6+}, not only showing the theoretical line but also showing the line for different values of L_a. b) Schematic representation of L_a

If we assume that the data we have now does not need to be scaled we still have this broad distribution around the theory line. One factor that might vary a lot is the origin point of the fragments. The factors in the equation is L_a, this is the distance from the origin to the edge of the acceleration region as can be seen in figure 28b.
In figure 28a we can see that large changes to L_a are taken but difference between them and our initial white curve is minimal. The changes to L_a taken here are not plausible and not even possible for the 2 L_a case. These values where taken because lower changes would be almost indistinguishable. We can clearly observe that L_a holds very little impact on the curve especially on the part of the spectra where we wore able to collect data. It is save to say that L_a fluctuations would not be a prominent factor in this broadening of our spectra.

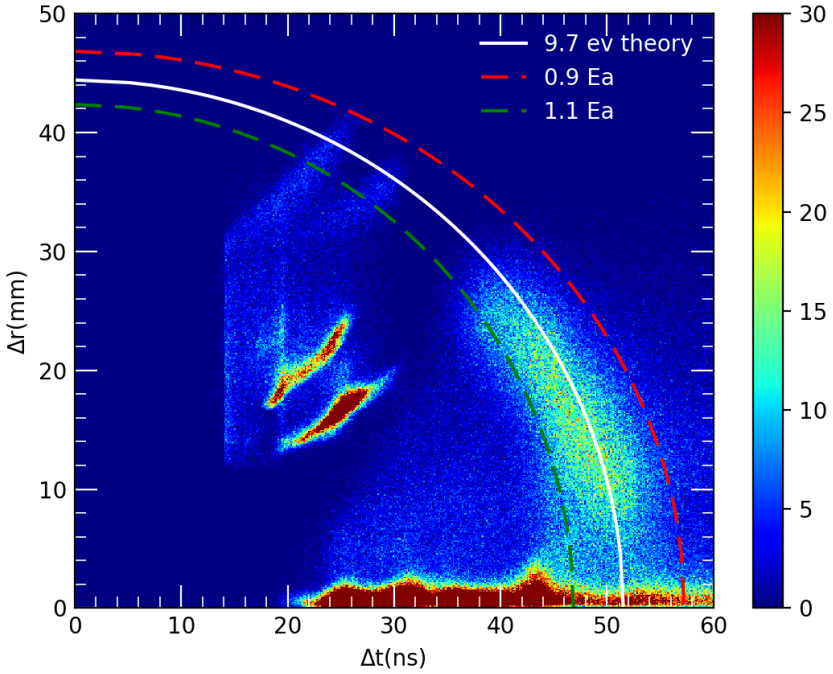

Figure 29: Coincidence of Sn^{6+}, not only showing the theoretical line but also showing the line for different acceleration field strengths

Another factor in the equations is the electric field strength of the acceleration field denoted by E_a. In figure 29 we can see the effect on the theoretical curves as Ea is changed. It shows that some fluctuations in the electric field might be the cause for the broad distribution. I do not believe there are actually 10% fluctuations in the electric field. I think it is more likely that the field is inhomogeneous meaning that the direction or size of the field is not everywhere the same. This could be caused by the plates possible becoming charged by the ions, edge effects of the electrodes, the electrodes not being completely symmetrical or fields with another origin somehow being present in the system just to name some. It might be an effect of the resistances that manage the voltage on the plates but the resistances of these differ only a small amount and I am not certain if this would even have a broadening effect since it should impact all of the fragments in that case.

One of the prominent factors that disturbs the data is the electrode with the notch which can be seen

in figure 24e. It is clear from that figure that it can both interfere with the position and timing data of particles in its proximity. Edge effect of the electrodes might thus play a role in these measurements. It is also not exactly known how far these effects extend into the opening. The exact effect and how many of the fragments are influenced by these effects is difficult to understand. We only found out about the edge effect of the plate with the notch due to the projectile beam traveling along it. The H^+ energetic particles might travel near other regions of the electrode due to the sideways momentum component meaning that many of the measured particles can be effect in some way by the edge of the electrode. This makes it seem like the edge of the electrode might have a huge effect on the spectra. We could replace the electrodes with the small inner radius for electrodes that have wider openings. This should reduce edge effect but might lead to a less homogeneous field which could of course increase broadening again. It might be better to introduce more electrodes on the positive side of the electrode stack to increase homogeneity. Robbert Julius has done simulations for these sort of situations[2].

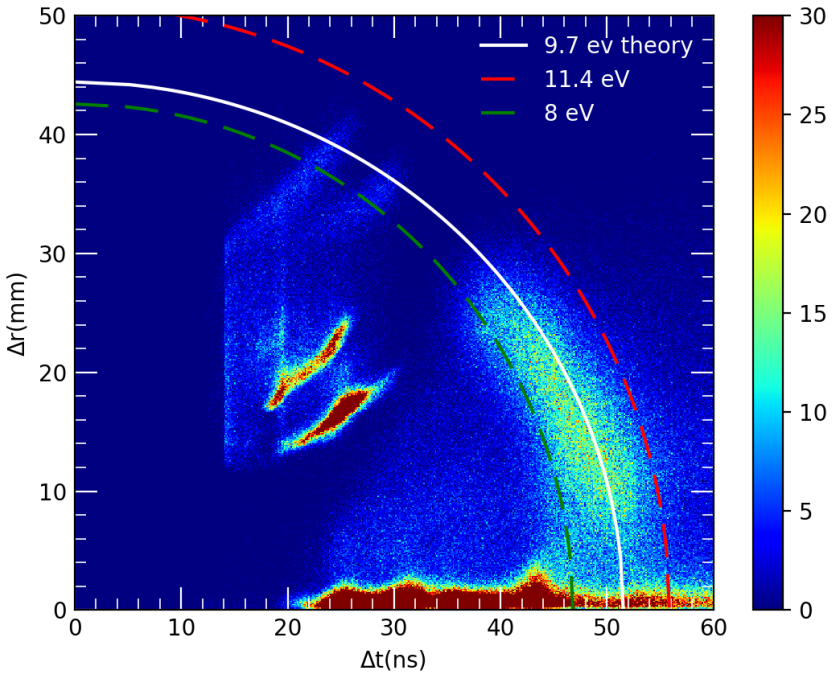

Figure 30: Coincidence of Sn^{6+}, not only showing the theoretical 9.7 eV line but also showing the line for 11.4 eV and 8 eV kinetic energy

Another possible option for this spread around the 9.7 eV line is the spread in energy that the H^+ will attain after double capture occurs. From figure 1 we can see that by utilising a Franck-Condon model the distribution of possible energies is quite large. We have made a plot that incorporates the energies near the edges of this energy distribution that arises using the Franck-Condon model, The plot can be seen in figure 30. We can actually see that the spread shows some agreement with these lines. Most of the hits are in between the lines. From the figure 1 it is clear that the distribution is not completely symmetrical and that the distribution allows for a higher ΔE at energies above 9.7 eV. Figure 30 shows that beyond 11.4 eV there are still some hits. This however does not mean much since this could simple be noise. If an additional filter is applied such that only H^+ will be shown in

the spectra we could preform a better analyses. The same holds for energies lower than 8 eV. There is to much noise present. My recommendation would be to make bins corresponding to energy ranges and see if we can find this same energy distribution as seen in figure .... theory2003..... If the data will fit this distribution nicely we could conclude that are setup is working very well and no problems with the of the field are present.
The pre-trigger problem could also lead to the broadening in the Δt but this should not be more than 3 ns as seen in figure 15. We do see that only a small amount of the hits suffer from the pre-trigger thus might not explain the intense broadening. It should however be fixed of course even if this is not the main factor causing the broad distribution. Another issue might of course be the accuracy of the detector. Roentdek gives an accuracy of < 0.1 mm[8] so this should not be a problem if the detector is working correctly.

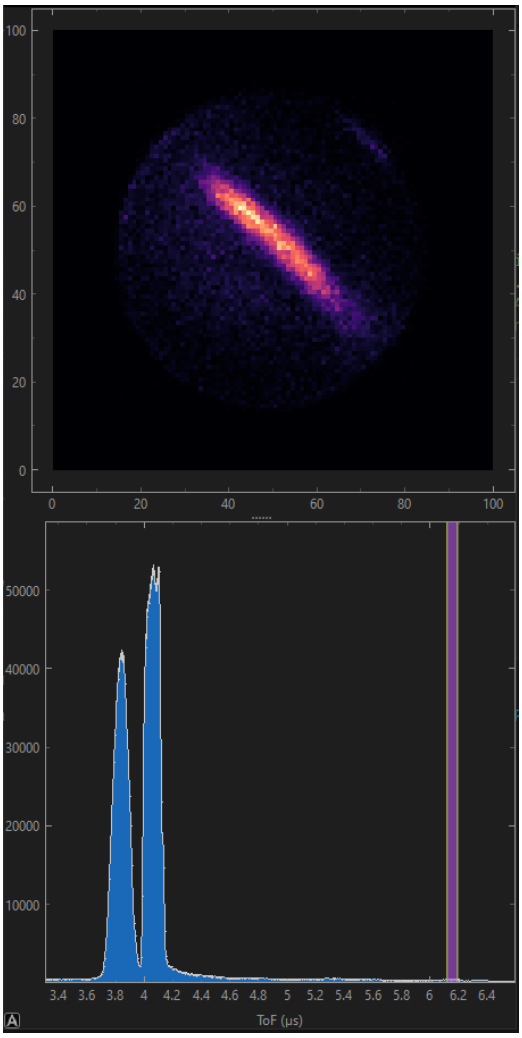

Figure 31: Position spectra of Sn^{6+} for a ToF window of an unidentified particle peak.The actual ToF window is shown below the position spectra

Another small remark is that after the main peaks we can observe some other very small peaks. These are most likely due to other particles than hydrogen since they arrive much later. One of these peaks can be seen in figure 31. The peak is small and will most likely not have any influence on the hydrogen measurements but could be interesting to look into for simply knowing what other processes are occurring in the reaction microscope. A few of these peaks can be seen in the Sn^{6+} spectra and seem to all be 0 eV interactions. The interactions with some energy might just not be as discernible because these peaks are already not very bright.

In figure 32 we can again see the position spectra for time since previous hit windows or Dt windows. The effect is similar to the spectra of Ar^{6+}. The spectra looks similar which might indicate that this is simply an effect of the electronics. It seems like it might be the MCP discharging while it is charging back up. Why this happens and why these square patterns appear is unknown. I can only imagine the square pattern being a product of some weird reflections over the MCP and might again be something that will improve when we attach the new MCP.

As a last note for this section I would like to discuss another graph that roentdek has included in their software cobold. It is the pipico graph which can be seen in figure 33. This graph gives us information about when the second hit hits the detector with respect to the first hit. First of all we notice the bright stripe near 3840 ns ToF first hit. This is the peak of H^+ which will give a lot of secondary hits because of the double capture producing two hydrogen fragments. We can also observe a bright stripe near 4200 ns ToF first hit. This stripe is due to the H_2^+ peak. H_2^+ does in principle not come in pairs so the brightness of this spot can only explained by re-trigger of the MCP or when multiple hydrogen-ion interactions occur in one chop. Multiple interactions occurring is also clear from the blue square observed between 3800-3900 ns ToF first hit and 4000-4100 ToF second hit. This square is formed because first a H^+ is detected followed by a slower H_2^+. If we want to minimise this effect we can lower ether the amount of Hydrogen gas present or the amount of ions present in a ion bunch. This can be done by simple letting in less hydrogen gas in to the system for the case of hydrogen. For the ions we can create a initial beam with less ions or make our ion bunch smaller by chopping the beam faster. All of these options will however also lower the speed of acquisition since now the chance of not having any interaction occur in a chop also increases. There also appear to be stripes in the spectra why these are present is unknown. It might be a result of the recharging mechanics of the MCP. We also observe some peaks in the Dt spectra of figure 32 which also have a separation of about 5 ns so these might come from the same origin. We could thus possible also remove these stripes from the pipico by using another MCP.

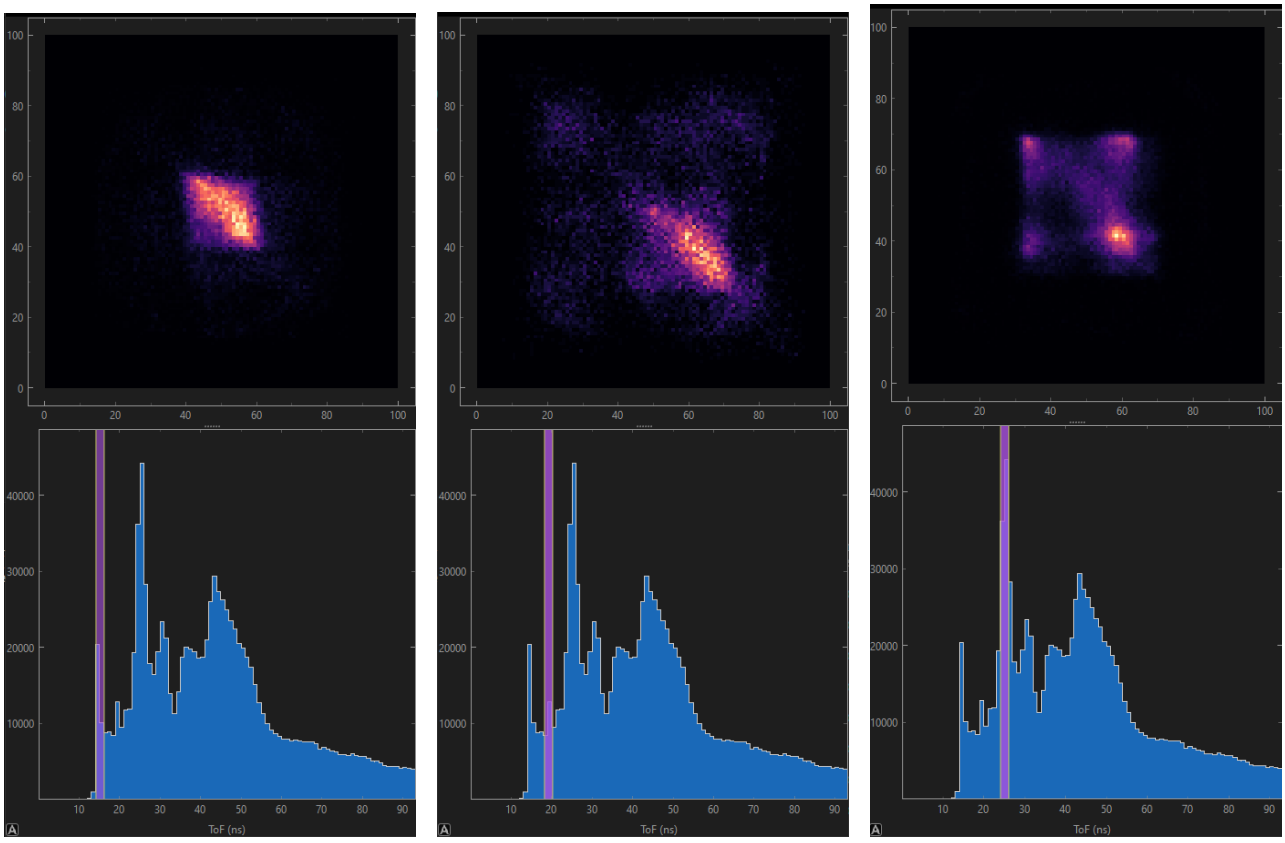

(a) (b) (c)

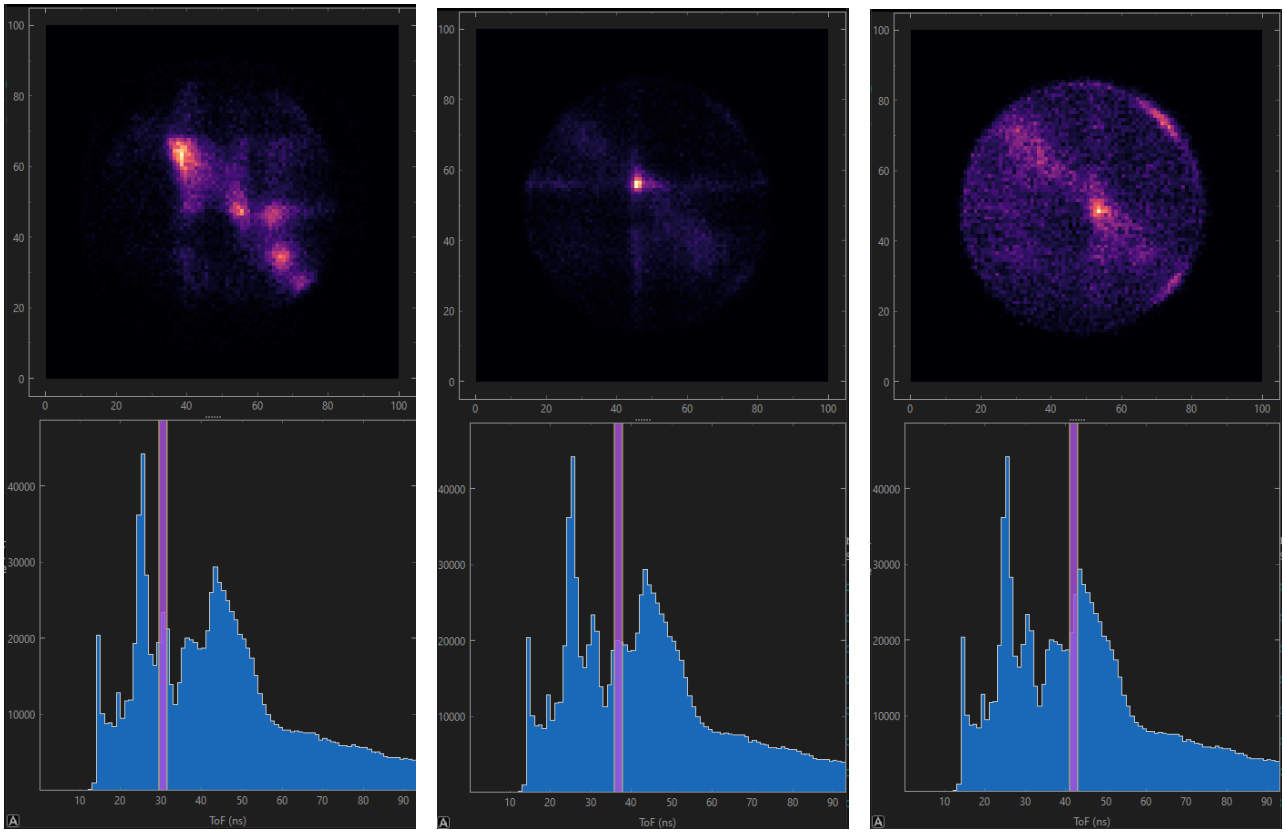

(d) (e) (f)

Figure 32: Position spectra of Sn^{6+} for Dt windows. The Dt increases for every figure. The actual Dt window is shown below the position spectra

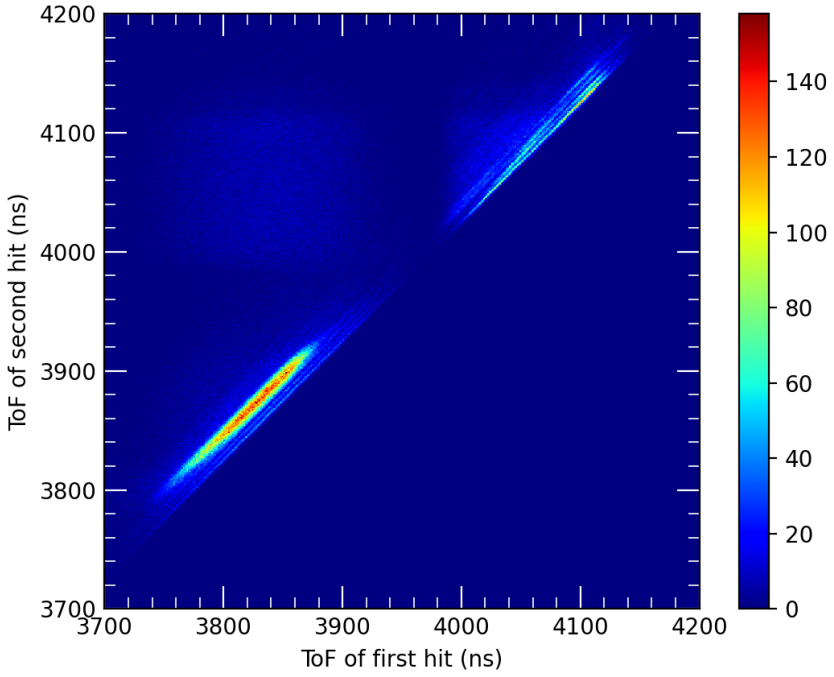

Figure 33: Pipico of Sn^{6+}, The x axis shows the ToF of the first hit in a group and the y axis shows the tof of the second hit. The graph only shows groups with at least 2 hits

4.5 He^{2+} 40 keV

In this section Results for the projectile ion He^{2+} are discussed. The new setup is used for these measurements and an extraction electric field of $8.7 \cdot 10^3 V/m$ by applying a potential of 500 V to the resistances that handle electrode voltages. The results here will also be compared to Sn^{6+} because they use the same setup

The Time of flight of He^{2+} can be seen in figure 34. We can again observe a clear H^+ and H_2^+ peak as we would also see in Sn^{6+} figure 22. We also see that the rise of the H_2^+ peak is very steep while the drop of the peak is less steep. This might be due to effect of the notch.

There are key differences between He and Sn spectra though. He is a lot lighter than Sn but they both have similar kinetic energy. This means that He is faster than Sn this is also visible in the H_2^+ peak being more narrow for He. To compare them visually I have shifted and normalised both of the peaks. they are shown in figure 35. This plot shows that the tin peak is much broader but also that He does not show as extreme an effect of the electrode edge on the spectrum. It is likely that the notch or edge causes the change in downward slope but has a less extreme effect than it had on the Sn because the He moves quickly past the notch. The full width half maximum of Sn is 130 ns and from He is 60 ns

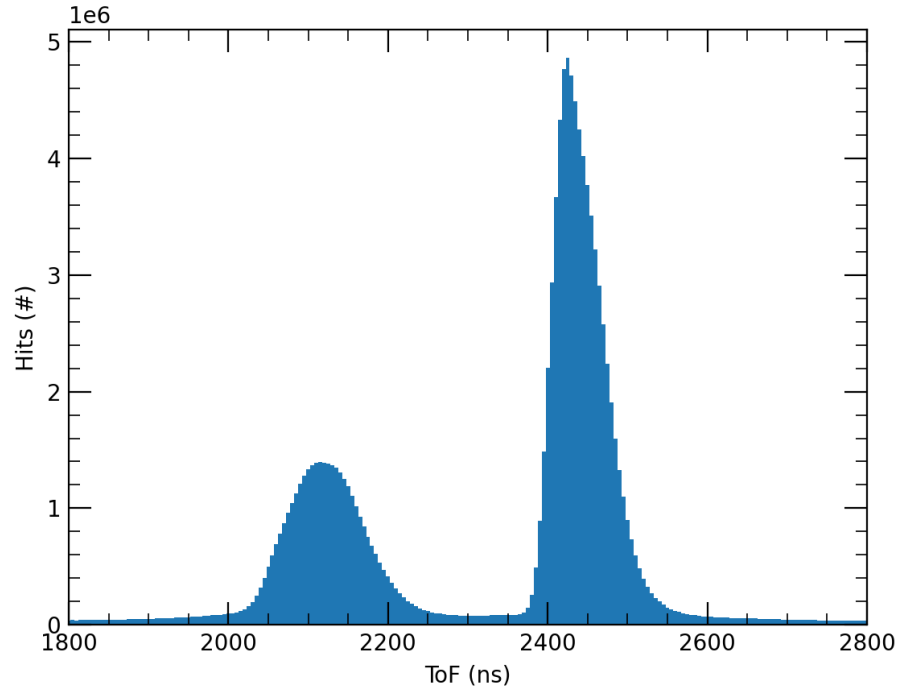

Figure 34: Time of flight spectra of hydrogen fragmets as a consequence of charge transfer with He^{2+}. The first peak corresponds to H^+ and the second peak corresponds with H_2^+

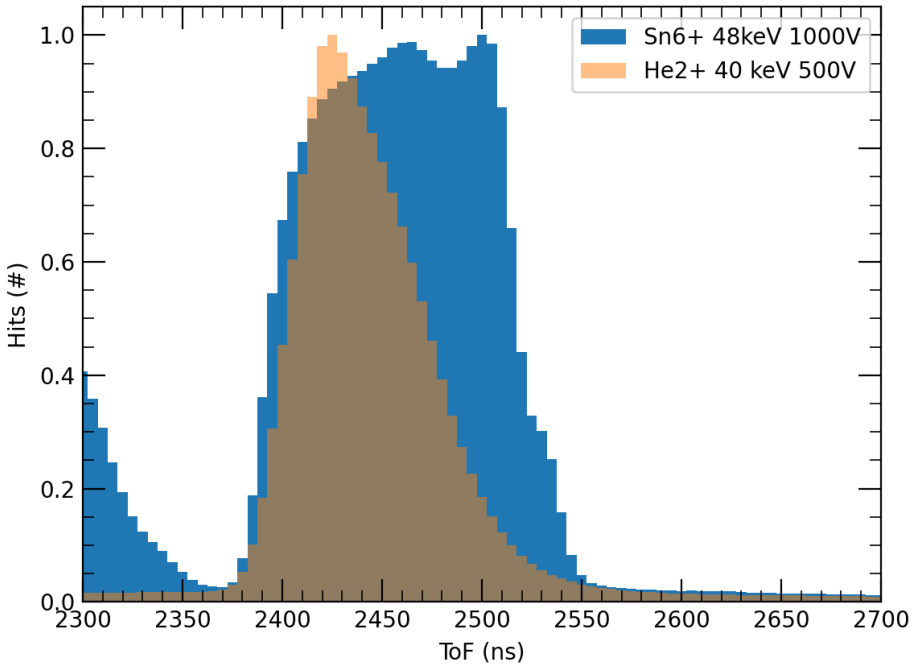

Figure 35: Time of flight of He^{2+} and Sn^{6+} normalised and shifted such that the H_2^+ peaks align

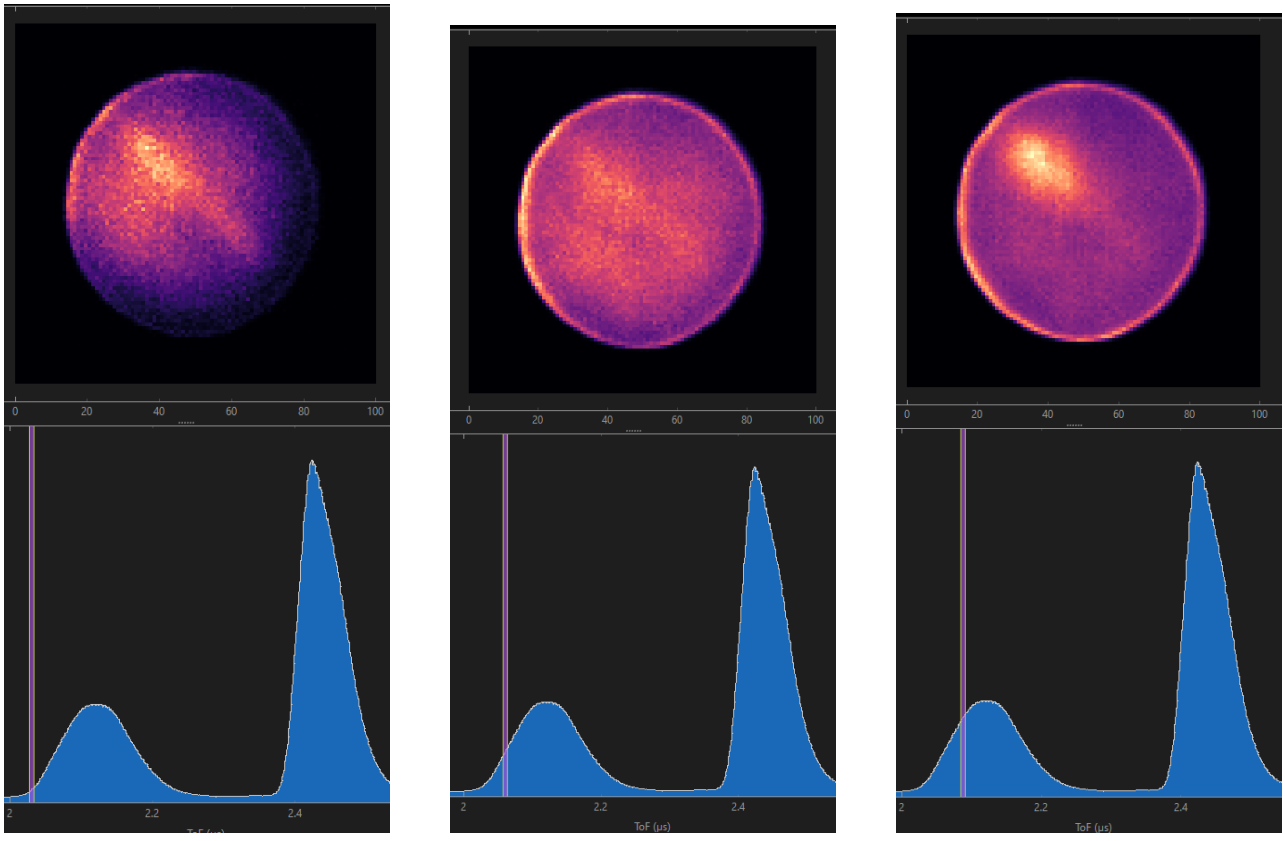

(a) (b) (c)

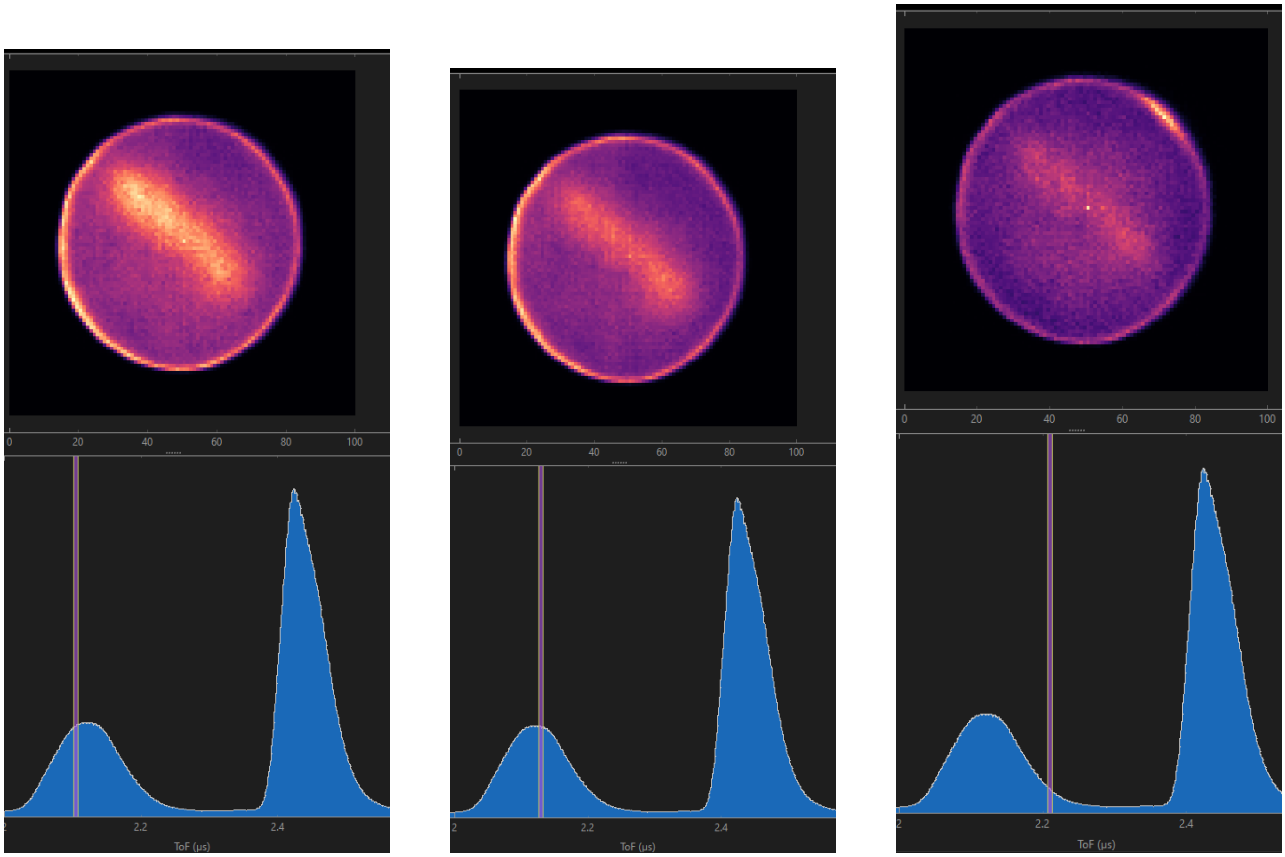

(d) (e) (f)

Figure 36: (part 1) Position spectra of He^{2+} for ToF windows of the H^+ peak. The ToF increases for every figure. The actual ToF window is shown below the position spectra

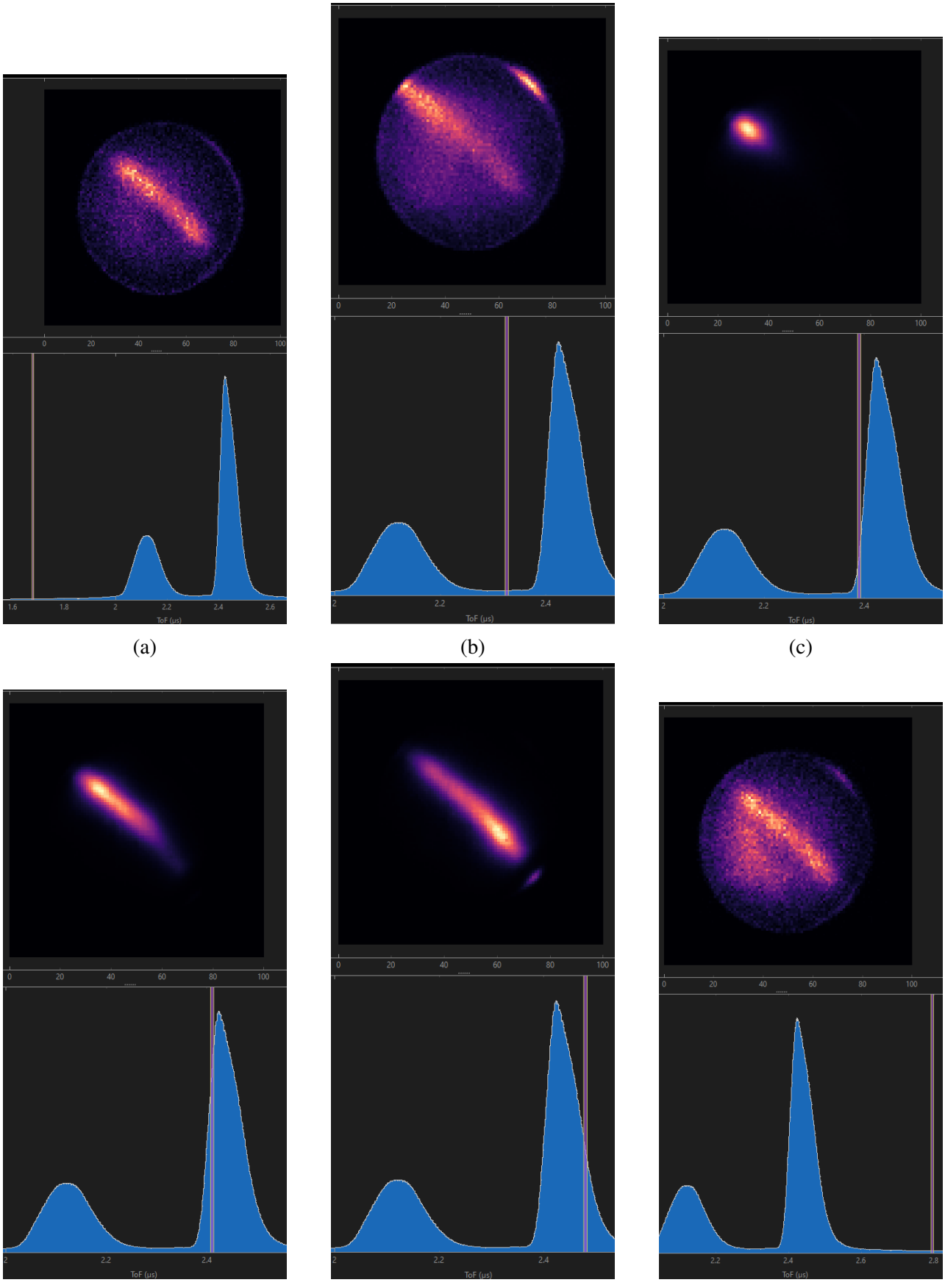

(a) (b) (c)

(d) (e) (f)

Figure 37: (part 2) Position spectra of He^{2+} for ToF windows of the H_2^+ peak and noise. The ToF increases for every figure. The actual ToF window is shown below the position spectra

The position spectra for specific ToF windows for He^{2+} can be seen in figures 36 and 37. The show similar results as for Sn^{6+}. We can again see H_2^+ coming in from the top left moving to down right in figure 37. We also observe a big distribution with the same trajectory for H^+. The important differences here are that the H^+ distribution is wider than it was for Sn^{6+} because of the lower field. This leads to more H^+ missing the detector which also explains that the H^+ peak is much smaller compared to the H^+ peak for Sn^{6+} in figure 22 where it is almost the same size as the H_2^+ peak. The Distribution also seems to have a more noticeable line similar to the H_2^+ spectra line. This might be due to the fact that much of the hydrogen with momenta now misses the detector thus the influence of H^+ of 0 eV becomes more pronounced and thus better visible than it was for Sn^{6+} with a higher field. The distribution also does not have as clear of a start and finish most likely due to the lower field strength. Another very noticeable difference is the speed of the H_2^+ peak. We can actually see that it quickly moves across the detector. We can again see the black spot at the bottom right due to most probably the electrode followed by the notch as in the Sn^{6+} section. Now one big feature of this spectra is a clear pattern in the noise region away from the peaks. We can see a stripe that follows the same path as the H_2^+ peak everywhere in the noise. It is difficult to say what caused this. We do not expect there to be a constant background with a pattern. It might be an effect of the MCP being triggerd a lot. Since the rate was very high for He it might lead the MCP to malfunction and produce random retriggers at random times. The interesting part of this is that it is also present before the peaks in the ToF meaning that the effect is than carried over from a previous chop. It could also be that the chopper is not bending the He^{2+} enough or deflecting it in a certain way that it can still move through the capillary allowing a small amount of hydrogen to constantly enter the reaction microscope. This is not necessarily a big problem since the actual peaks are still way bigger than the noise.

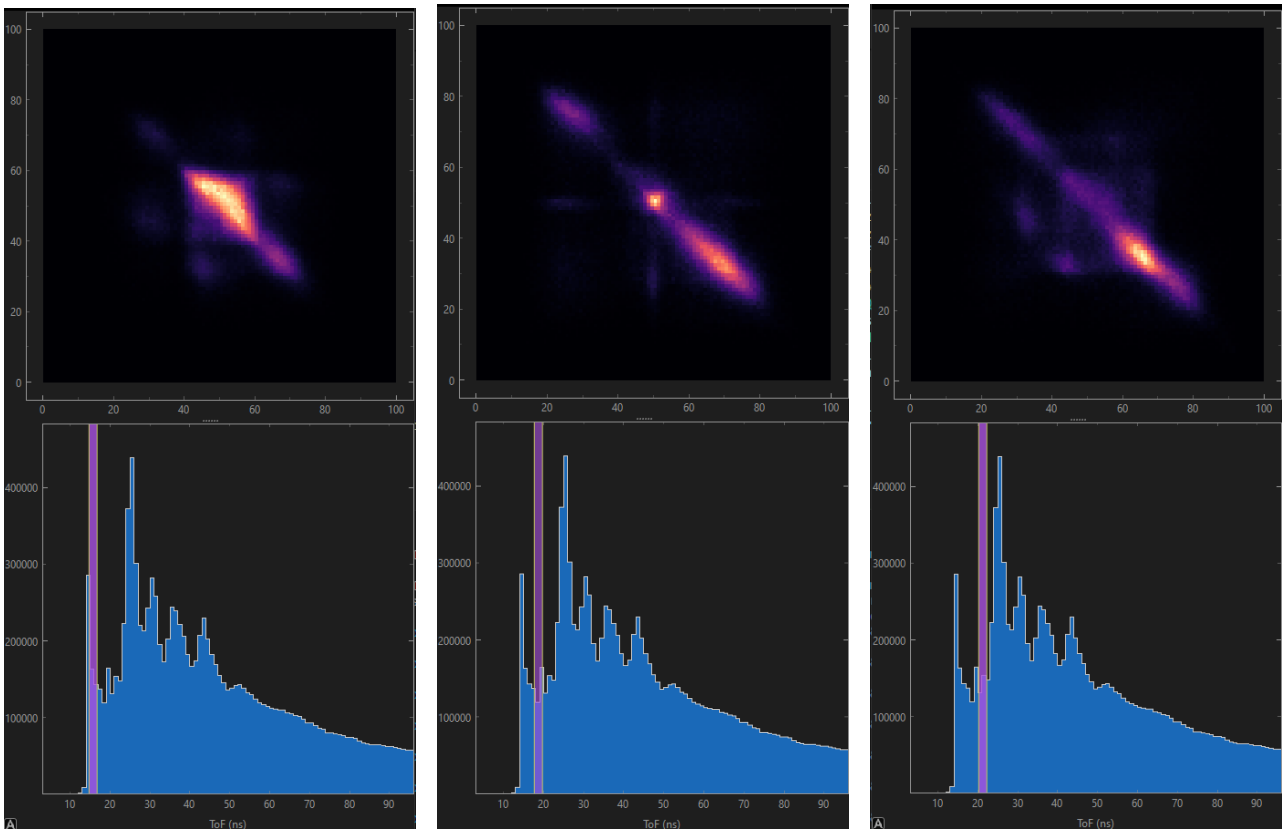

(a) (b) (c)

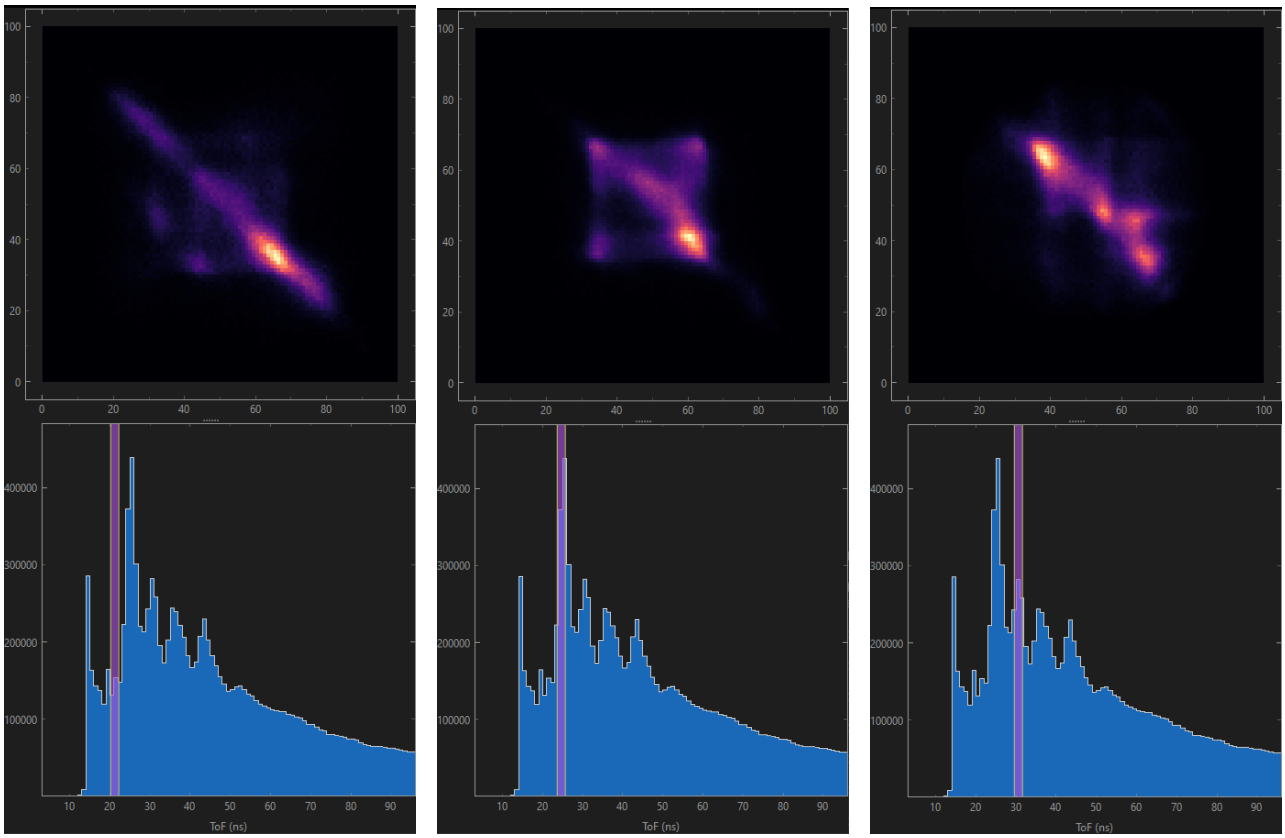

(d) (e) (f)

Figure 38: (part 1)Position spectra of He^{2+} for Dt windows. The Dt increases for every figure. The actual Dt window is shown below the position spectra

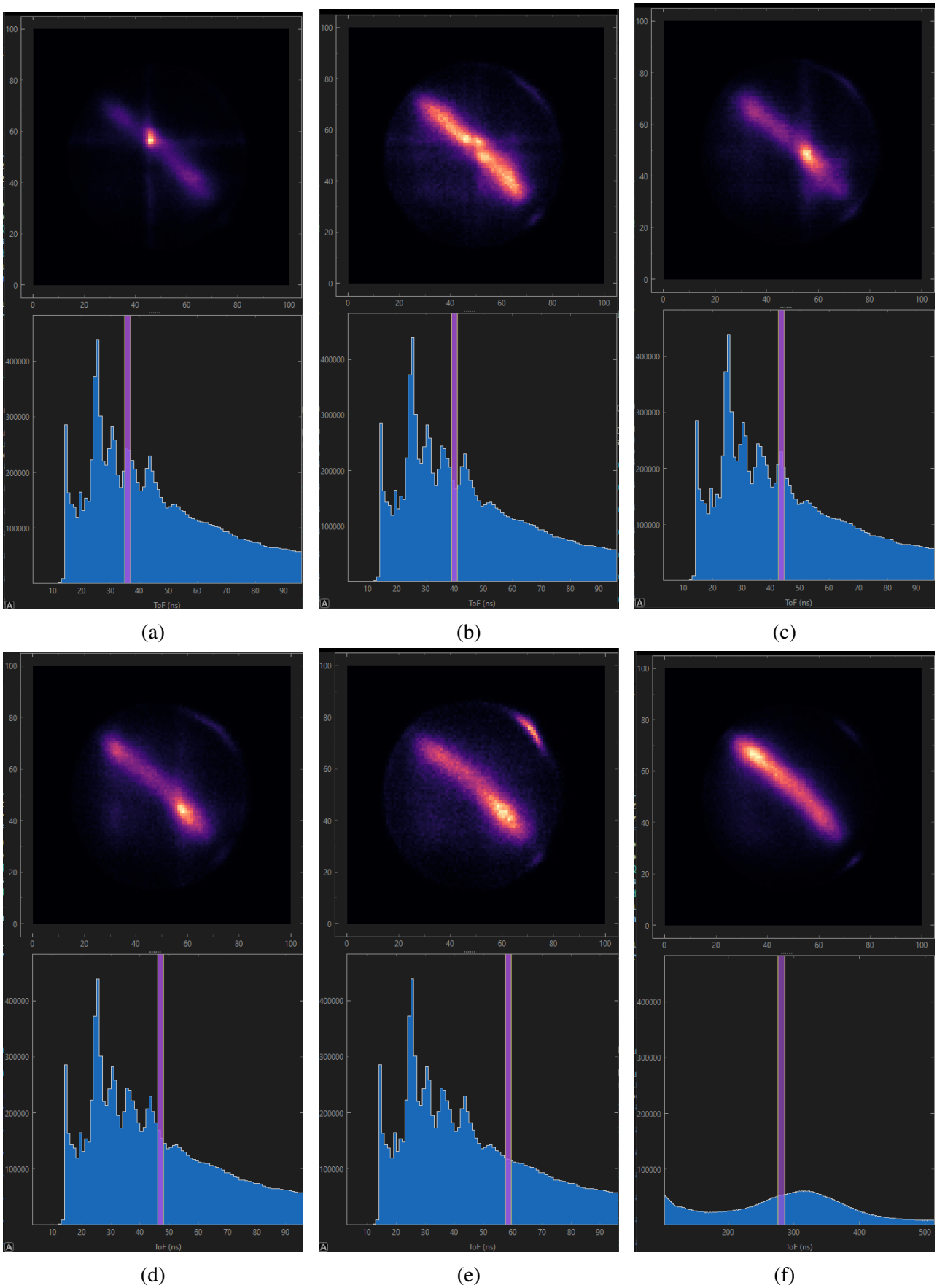

Figure 39: (part 2)Position spectra of He^{2+} for Dt windows. The Dt increases for every figure. The actual Dt window is shown below the position spectra

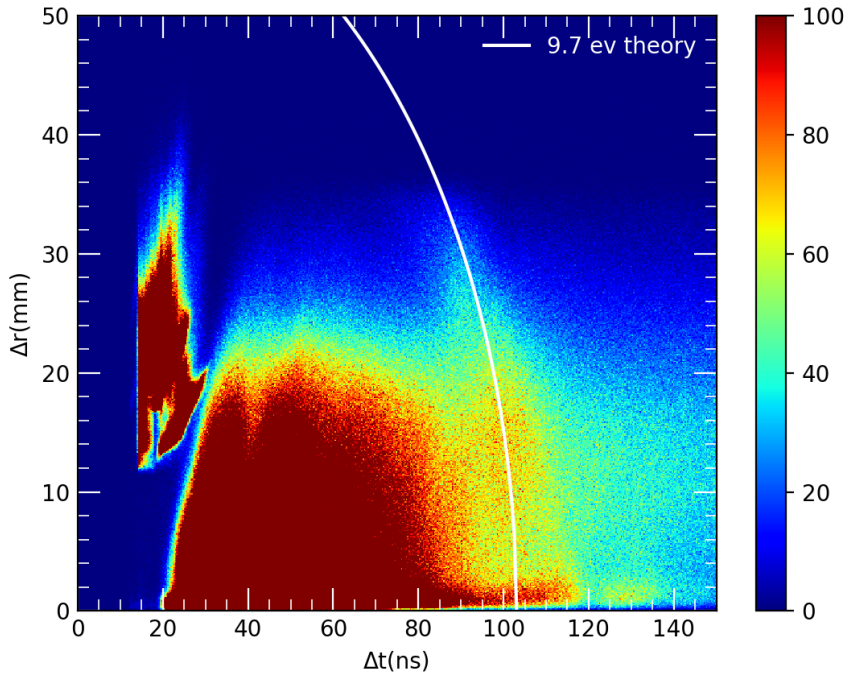

Figure 40: Coincidence of H ions with He 2+ projectile ions of 40 keV, Δt is the time between subsequent MCP hits in one group, Δr is the position difference on the delay lines between these same hits, The white line corresponds to what theory predicts, the colors corresponds to the amount of hits

The position spectra for Dt windows of He^{2+} are shown in figures 38 and 39. We observe the same patterns again here as we saw for Ar^{6+} and Sn^{6+}. The position spectra shows some patterns and the Dt spectra has some peaks spaced by about 5 ns. The spectra only seems to return to a more expected shape at around 60 ns. Here all of the artifacts in the position spectra are gone and the peaks of the Dt are also not present anymore. The spectra than shows a 0 eV position spectra. This was also present for Sn^{6+} but not as clear. This reveals that more H_2^+ secondary hits are registered than was the case for Sn^{6+}. This is likely because there are more ions in every He bunch leading to a higher chance of uncorrelated secondary interactions to occur. There is also a peak near 300 ns as seen in 39f. This is likely a peak coming from secondary H_2^+ where the first hits come from H^+. This same 300 ns difference can be calculated by filling in equation 15 for both H^+ 0 eV and H_2^+ 0 eV and subtracting. The spectra could still be improved by only selecting data points in the H^+ peak since this would remove the effect of the secondary triggers caused by the H_2^+ peak

The coincidence measurement of the hydrogen fragments with He^{2+} as projectile ions can be seen in figure 40. If compared to 25 it becomes apparent that there are more hits in the area before the theory line, around 20 to 80 ns. This is most likely due to the higher amount of interactions in one ion bunch for He. We can also notice that the theory line is different for He due to the lower electric field. The distribution is still present around the line from theory as before for Sn. It cuts off around a similar Δr. The cutoff for He seems to be a bit higher but not by more than about 5 nm and the intensity near the cut off is very low which might just mean that it is very improbable to happen. We can tell from this picture that the Δt might also be a limiter.

From 20 ns there is a diagonal cut off. This cut off might be due to the way signals are processed. As discussed in section 3.3.2 a first and a second ion will not be handled properly if the hits are not received in a set order. If some of the first hit signals arrive after there respective second hit signals the time sum will not be constant and thus the measurement will be scrapped. Losing the measurement in the process. There could also be a set dead time on the CFDs which seems to be 20 ns in this case. If we take take the wire loop pitch of the DLD to be 0.75 ns/mm[8] than we expect our 40 mm to take 30 ns. If we add the 30 ns and 20 ns to get the cut off for measurements taken from opposite sides of the detector we would expect the max cutoff to be 50 ns although the cut off appears to happen sooner. If we combine this thought process with a previously made observation that our MCP might be smaller than expected and actually has a diameter of about 30 mm. The travel time across the entire diameter will than be 22.5 ns. We than obtain 42.5 ns as maximum cut off. This seems to roughly align with the cut off for the He spectra. Some simplifications are made here. We have not taken the actual loop pitch in mind and the difference between the loop pitch for x and y are also not taken into account. This however seems to give an understanding of this cutoff line in the spectra. The problem with this theory is that there are still measurements below 20 ns. These are on an island next to the cut off. There should still be a reason found for this island. The same cut off behaviour shown for He is also observed for Sn but here the cut off is less apparent due to less random hits. Another strange phenomena is that the distribution around the theory line seems to go slightly beyond the cut off line in figure 25. The only possible explanation for this would be that the cut off is just not very clear due to the low amount of data there. To lower this dead time between hits it could be a good idea to revise hit detection logic. We could for instance not remove measurements with incorrect time sums right away but wait if there are any additional hits shortly after the initially received ones. We could than try combinations of these hits to match a correct time sum. In this way we should be able to extend the range of our data acquisition and detect more of the low Δt high Δr ion pairs.

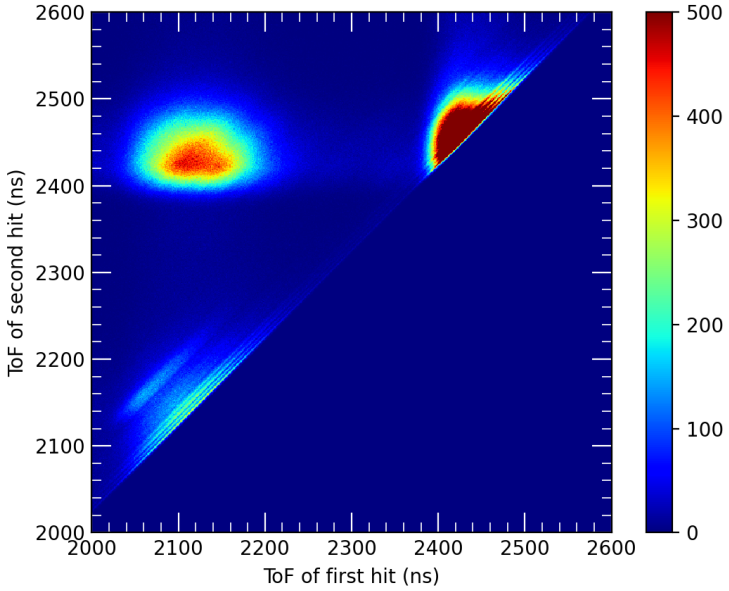

Figure 41: Pipico of H ions produced by He^{2+} projectile ions of 40 keV, The x axis shows the ToF of the first hit in a group and the y axis shows the tof of the second hit. The graph only shows groups with at least 2 hits

The pipico of H ions produced by He^{2+} projectiles can be seen in figure 41. The graph shows the same general features as was the case for Sn but shows that the area where first hits coming from H^+ and second hits coming from H_2^+ (top left area) is more pronounced. This shows us again that many ion bunches undergo multiple uncorrelated processes. As discussed before we would want to reduce this effect. We can also again see the stripes going through the H^+ and H_2^+ peak also visible for Sn in figure 33 This figure however also shows that these are not present for the top left area indicating that these stripes could be tied to the time difference between hits. This is another reason to assume that the peaks in the Dt graphs have the same origins as the stripes in the pipico since these are both not present at higher time differences.

5 Conclusion

The project has been a success. We where able to produce data that matches the theoretical predictions. The results did not turn out as initial simulations had shown because of a inaccurate assumption of a small interaction region which in reality coincides with the entire ion beam path through the acceleration region. Coincidence proved to be an effective method of checking energy of the coulomb repulsion of hydrogen fragments produced by double capture and first data suggests this value is 9.7 eV as theory predicts. There are however still many possible improvements that can be made.

First of all the coincidence spectra can be cleared up by simple selecting only the data that should show coincidence. This means that only data from the H^+ peak should be used for the coincidence. This filter can be applied to all the hits since a first hit of H^+ and a second one of H_2^+ would also not be useful. I would suggest making the accepted region a bit larger than the clearly visible H^+ peak especially for the area behind the peak since second hits of H^+ tend to have a bit of a shifted peak with respect to the total H^+ peak.

Many of the problems that where found with the setup might be due to the current MCP stack. Such as the MCP possible being smaller than 40 mm in diameter. As well as unexpected artifacts in many of our spectra like periodic stripes in pipico, peaks in Dt time spectra and geometries in Dt position spectra. The MCP also seems to suffer from accidental retriggers as is clearly apparent by the line along the dead time of the pipico plots. All of these possible problems combined with the fact that the new MCP is not stored in an adequate environment which will only deteriorate the quality of the MCP over time leads me to think that the best option is to replace the current MCP with the new one.

If we would like a coincidence spectrum that shows more of the full curve we will need to work on the dead time and hit logic in the system. Implementing a hit logic system that will check for a correct time sum of different hit combinations instead of only the first one that arrive should help with detecting hydrogen fragments with a large parallel momentum component. Cobold also has some dead times set by software which might not be necessary. If we create our own software to control and read out the electronics we might be able to further reduce dead times.

The constant background in the shape of 0 eV particles in the He^{2+} spectra should also be investigated. Using a higher potential difference between the chopper plates should have an impact on the effect. The effect was far less noticeable if present at all for Sn^{6+} so it might not be a big problem for further Sn measurements. It would be wise to always check if this background is present because it will slightly impact the data.

The theory could possible explain the spread around 9.7 eV in the coincidence data. This could be due to the nature of the wave function of the hydrogen molecule transitioning into energetic hydrogen fragments due to double capture. A logical next step would be to bin energy ranges to see if the energies follow the same distribution as the Franck-Condon model shows for this transition. These results could be of great importance to further experiments since if the spread comes from theory it would mean that the electrode plates will probably not have to be replaced. If this distribution does follow the Franck-Condon model we could start experiments with Sn^{3+} as projectile ion. This ion showed an unusually low energy of the H^+ fragments in previous measurements. The complete energy distribution might lead to new insides in its double capture mechanism.

One of the important challenges of the setup is reducing the spread around the theory line such that we would be able to fit the energy through the data without a big error. It seems likely that an inhomogeneous electric field is causing at least some of this spread. Since we where able to observe how much of an effect the electrode edge had on the H_2^+ peak it seems likely that this could also have influence on our H^+ data. Our main concern is the coincidence data. For two H^+ to be detected in coincidence they should originate from the area in front of the detector and not come from the area outside the acceleration region. We might thus be able to remove data that hits near the edge of the detector to reduce the amount of spread due to edge effects in the data. This would not be ideal since the detector area is already small and the area we would have to remove from the data does not seem to leave a lot of detector space left.

We might thus want to consider a different approach. We could increase the inner diameter of the electrodes near the beam entrance and use a setup with the same electrode plates everywhere. We might want to add more positive electrodes to ensure that the field is still homogeneous around the interaction region. This change would reduce the effect of the edge probably but it might still not remove them for all the H^+ particles. We could than still use the idea of removing data in a small area around the edge of the detector to further reduce the broadening. It might be useful to run more simulations for the current and this new electrode stack to check the homogeneity of the field. Before deciding if this will be necessary I recommend to first look into the energy distribution and see if this is already in agreement with the Franck-Condon model

If we would want to reduce all edge effects in our coincidence we might want to create a bigger set up as a whole. If we would use larger electrodes with bigger holes it would be unlikely that any coincidence measurements will suffer from edge effects. The reason to do this is to create a more homogeneous field thus simulations should be done to determine if larger diameter plates with larger holes produce a homogeneous field. It should also be taken into account that the vacuum chamber does not allow much larger plates than currently used. So this might not be the ideal option unless we are also interested in changing the vacuum chamber.

We could use a bigger detector such that we can detect all possible hydrogen trajectories. We could than maybe also decrease the field leading to improved time and position resolution. An important note to be made is that a bigger delay line detector also introduces a larger wire pitch which would increase the likelihood of problems with hit logic for position detection that we discussed before. If we are not able to solve the problem with the hit logic, a bigger DLD might harm the results. If we would like to upgrade to a larger detector we would have to see if the change to lower fields makes up for the increased dead time at high Δr, again assuming we are not able to solve the hit logic problem.

Bibliography

[1] S. Rai, *Ionic interactions around EUV generating tin plasma*. PhD thesis, University of Groningen, 2023.

[2] R. Julius, "Schemes, procedures and design considerations for measurements of energy-transfer and momentum-transfer during snq+-h2 collisionss," 2023.

[3] T. Sharp, "Potential-energy curves for molecular hydrogen and its ions," *Atomic Data and Nuclear Data Tables*, vol. 2, pp. 119–169, 1970.

[4] S. H. Martínez, G. C. Bernardi, P. R. Focke, A. D. González, and S. Suarez, "H2 dissociation by h+ and he2+ projectiles at intermediate energies," *Journal of Physics B*, vol. 36, pp. 4813–4826, 2003.

[5] R. Dörner, O. Jagutzki, S. Nüttgens, V. Mergel, L. Spielberger, K. Khayyat, T. Vogt, H. Bräuning, K. Ullmann, R. Moshammer, J. Ullrich, S. Hagmann, K.-O. Groeneveld, C. Cocke, and H. Schmidt-Böcking, "Multi-hit detector system for complete momentum balance in spectroscopy in molecular fragmentation processes," *Nuclear Instruments and Methods in Physics Research Section B: Beam Interactions with Materials and Atoms*, vol. 149, pp. 490–500, 03 1999.

[6] O. Jagutzki, "The roentdek constant fraction discriminators cfd8c, cfd7x, cfd4c, cfd1c and cfd1x," *Roentdek handels GmbH*, p. 26, 2021.

[7] J. Ladislas Wiza, "Microchannel plate detectors," *Nuclear Instruments and Methods*, vol. 162, no. 1, pp. 587–601, 1979.

[8] O. Jagutzki, "Mcp delay line detector manual," *Roentdek handels GmbH*, p. 114, 2024.